Photocatalytic Splitting of Water

Nathan Skillen, Cathy McCullagh, and Morgan Adams*

IDEAS, Institute for Innovation, Design and Sustainability Research, CREE, Centre for Research in Energy and the Environment, The Robert Gordon University, School of Engineering, Aberdeen, AB10 7QB, UK

**Corresponding author: Tel; 01224 262826, email address; n.c.skillen1@rgu.ac.uk*

Keywords: Photocatalysis, photoelectrochemistry, water splitting, semiconductors, photoreactors

Abstract

The use of photocatalysis for the photosplitting of water to generate hydrogen and oxygen has gained interest as a method for the conversion and storage of solar energy. The application of photocatalysis through catalyst engineering, mechanistic studies and photoreactor development has highlighted the potential of this technology, with the number of publications significantly increasing in the past few decades. In 1972 Fujishima and Honda described a photoelectrochemcial system capable of generating H_2 and O_2 using thin film TiO_2. Since this publication, a diverse range of catalysts and platforms have been deployed, along with a varying range of photoreactors coupled with photoelectrochemical and photovoltaic technology. This chapter aims to provide a comprehensive overview of photocatalytic technology applied to overall H_2O splitting. An insight into the electronic and geometric structure of catalysts is given based upon the one and two step photocatalyst systems. One step photocatalysts are discussed based upon their d^0 and d^{10} electron configuration and core metal ion including transition metal oxides, typical metal oxides and metal nitrides. The two step approach, referred to as the Z-scheme, is discussed as an alternative approach to the traditional one step mechanism and the potential of the system utilise visible and solar irradiation. In addition to this the mechanistic procedure of H_2O splitting is reviewed to provide the reader with a detailed understanding of the process. Finally, the development of photoreactors and reactor properties are discussed with a view towards the photoelectrochemical splitting of H_2O.

Contents

1 Introduction

1.0 Historical overview of water splitting

The production of renewable and non-polluting fuels via the direct conversion of solar energy into chemical energy remains a fascinating challenge for the end of this century. Among various interesting reactions, the splitting of water into molecular hydrogen and molecular oxygen by visible light is potentially one of the most promising ways for the photochemical conversion and storage of solar energy (Maeda *et al.* 2005; Lee *et al.* 2007; Bard 1979; Sayama *et al.* 2001). Since the first reported photo splitting of water by Fujishima and Honda in 1972 many authors have published their efforts to split water using semiconductor photocatalysis (Bolton 1996; Esswein and Nocera 2007; Kudo and Miseki 2009; Amouyal 19995).

Photocatalytic water splitting was first reported by Fujishima and Honda in 1972 where they used TiO_2 thin film as the photocatalyst. Since then, TiO_2 has become a widely used photocatalyst in photocatalytic water splitting. Nevertheless, the biggest disadvantage of TiO_2 is its inability to harvest the visible light which accounts a major portion of sunlight. To overcome this shortcoming, several techniques, such as metal doping, ion doping, and dye sensitization, have been studied extensively (Dvoranova *et al.* 2002; Ikuma *et al.* 2007; Jin *et al.* 2007). Despite the successful development of several visible-light driven photocatalysts, only low hydrogen or oxygen production yield can be obtained, which is attributed to the intrinsic bandgap limitation of the photocatalyst.

This chapter aims to give an insight into photocatalytic technology applied to H_2O splitting for the production of H_2 and O_2 covering the areas of catalysts development, mechanistic pathways and reaction chambers deployed. A comprehensive, yet not exhaustive review has been compiled to provide the reader with an understanding of the fundamentals of this field of research. The topics covered herein include a review of one- and two-step photocatalysts, the mechanism of H_2O splitting and a brief overview of photoreactors including photoelectrochemical cell typically used for the production of H_2 and O_2.

1.1 Important parameters to be considered for water splitting

The following chapter is written with a view towards overall H_2O splitting and as such a number of parameters, put forward by Kudo and Miseki in their review in 2009, should be considered when reviewing published work in the field. There are additional parameters which are discussed in review papers (Kudo and Miseki, 2009; Ohtani, 2008), however, detailed below are the key parameters:

1. Stoichiometric production of H_2 and O_2
2. Experimental time frame

3. The turnover number (TON)
4. Quantum yield
5. Photoresponse

The stoichiometric production of H_2 and O_2 should follow the ratio of 2:1 respectively in the absence of a sacrificial reagent. Often reported is the evolution of H_2 in the presence of a sacrificial reagent with minimal O_2 recorded. It is ambiguous as to whether this is overall H_2O splitting and not a sacrificial reaction.

The evolution of H_2 and O_2 should be directly proportional to time and should increase with an increasing irradiation time. The production of H_2 and O_2 should also be stable over the time course with evolution occurring after the system has been evacuated.

The turnover number (TON) refers to the production of H_2 and O_2 in relation to the photocatalyst. In overall H_2O splitting the production of H_2/O_2 should be significantly greater than the amount of catalyst deployed. If the quantity of H_2/O_2 is less than the amount of catalyst it is not clear if the process has occurred photocatalytically. The TON is typically defined as the ratio of the number of reacted molecules to the number of active sites. As the number of active sites for a photocatalyst is difficult to establish the TON is often calculated by the ratio of number of reacted electrons to the number of atoms in a photocatalyst or number of atoms at the photocatalyst surface. The number of reacted electrons can be established from the volume of H_2 evolved.

Variation in experimental conditions presents a problem in the comparison and review of data. While the majority of data is presented as a unit such as $\mu mol\ h^{-1}$, photocatalytic activity is dependent on conditions such as irradiation source and reactor geometry. As such the quantum yield is an important parameter to evaluate. The determination of the number of absorbed photons by a photocatalyst is difficult to ascertain, therefore the calculated quantum yield is referred to as the apparent quantum yield (AQY). The AQY is calculated as the ratio of the number of reacted electrons to the numper of incident photons.

The response which is initiated by the absorption of light energy greater than the band gap of the catalyst should be evaluated especially when using a visible light catalyst. This can be achieved by using suitable control experiments which monitor H_2O splitting in the absence of a catalyst or illumination. Cut-off filters should also be used with visible emitting lamps to ensure activity being recorded is a result of the catalyst being excited by visible light photons.

Taking into consideration the above mentioned parameters there is a general trend which indicates H_2O splitting results are reliable, Figure 1. Reliable data should show steady stoichiometric evolution of both H_2 and O_2 with no activity prior to illumination and no significant deactivation of the catalyst

over an increasing time frame. In contrast, unreliable data shows activity which could not be attributed to photocatalytic activity such as H_2 evolution under no illumination and lack of O_2 evolution.

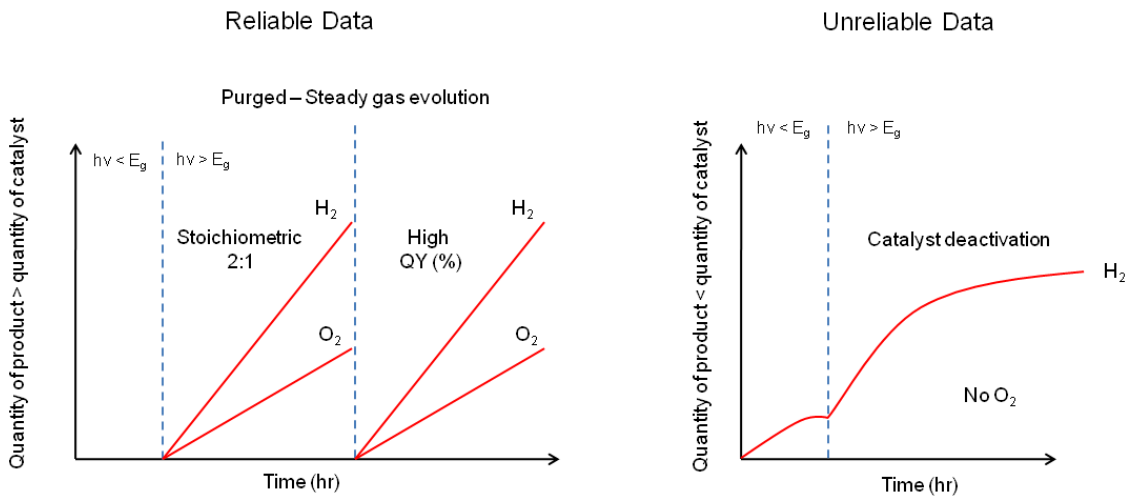

Figure 1; Comparison of typical reliable and unreliable data for H_2O splitting

2 Photocatalysts for water splitting

Water splitting over photocatalysts can be divided into two broad categories. The initial approach is the one step photocatalyst stage, during which a catalyst is exposed to light to generate the production of H_2 and O_2. This approach requires the photocatalyst to have sufficient thermodynamic potential to allow the splitting of water. Ideally it would also require a catalyst to have a narrow band gap to allow excitation by visible photons and have sufficient stability to prevent photo corrosion. The second approach uses a two photocatalyst system, modelled on the photosynthesis process. The system is referred to as the Z-scheme.

When considering powdered photocatalysts for H_2O splitting a significant level of focus is given to transition and typical metal oxides and nitrides. Figure 2 details common elements which are used to compose photocatalysts for H_2O splitting. The red and green highlighted elements are transition and typical metals respectively, while the blue highlighted elements are those that are frequently used as dopants and co-catalysts in photocatalytic complexes.

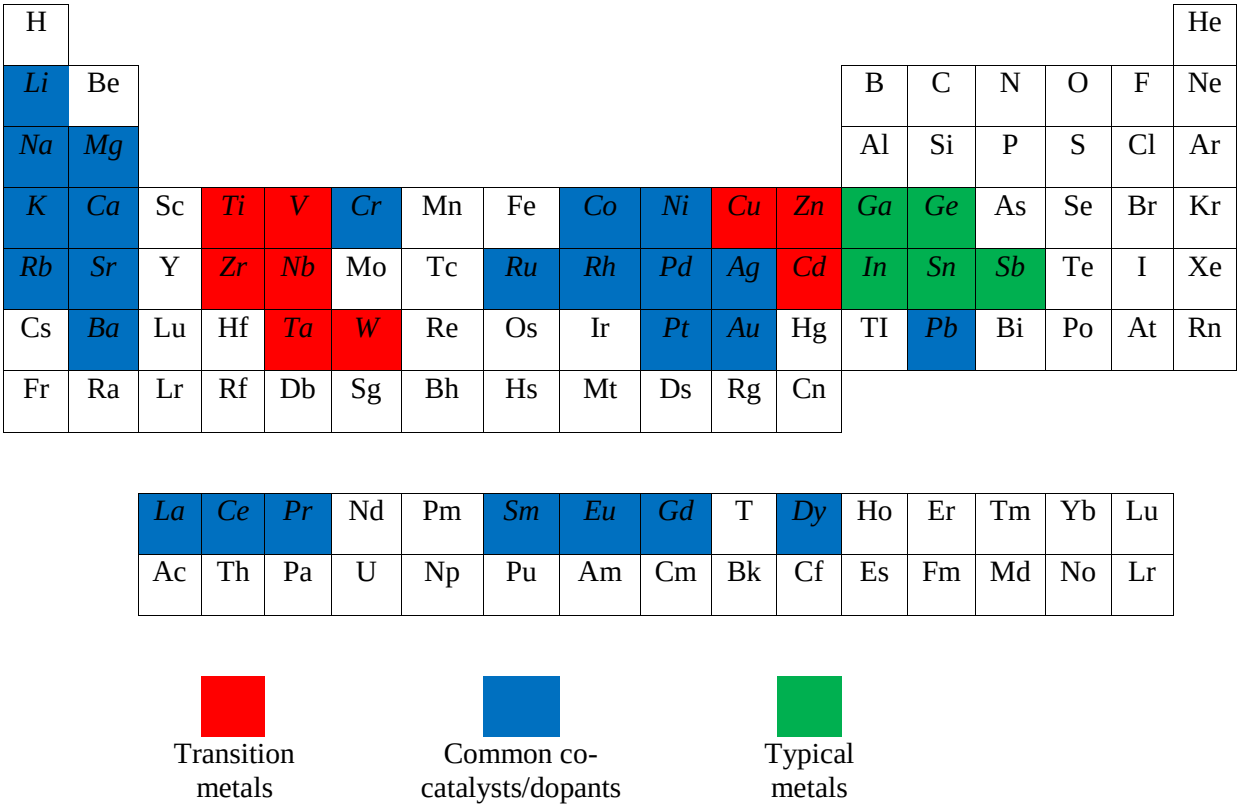

Figure 2; Periodic table highlighting common elements used in H_2O splitting catalysts

It is the electronic configuration of catalysts which make them suitable for photocatalytic mechanisms. Transition metal oxides with a vacant d orbital (d^0 configuration) primarily include titanates, tantalates, niobates, vanadates and tungstanates. Typical metal oxides have shown photocatalytic H_2O splitting activity with an occupied d orbital (d^{10} configuration). Inoue (2009) made the observation that d^0 and d^{10} configurations on a quantum chemistry level behave in a similar fashion. Catalysts with d^{10} configurations include gallates, germanates, stannates, antimonates and indates.

The catalysts discussed here are grouped firstly on their electronic configuration and secondly on the core metal ion of the compound. Within these groupings the geometric and electronic structure, distortion and performance of the catalysts are discussed. An overview of selected catalysts is also provided in Table 1, however, the reader is encouraged to refer to a number of excellent review papers which provide a detailed insight into catalyst development (Kudo and Miseki, 2009; Inoue, 2009; Moriya *et al.* 2013; Maeda, 2011; Abe, 2010).

2.0 Water splitting over powder photocatalysts

The photocatalytic decomposition of H_2O over semiconductor powders has been studied for the conversion of photon energy into chemical energy. Thermodynamically, the photocatalytic splitting of H_2O into H_2 and O_2Equation (1) is described as an 'uphill reaction' where a large positive change in the Gibbs free energy is observed (ΔG_o = -238 kJmol^{-1}) (Maeda, 2011). The properties of a catalyst including the positioning of the conduction band (CB) and valence band (VB) can dictate the level of activity. The CB of the catalyst must be more negative than the reduction potential of H^+ to H_2 (0 eV vs NHE at pH 0), Equation (2). The VB must also be more positive than the oxidation potential of H_2O to O_2 (1.23 eV vs NHE) (Maeda, 2011), Equation (3).

$$2H_2O \rightarrow 2H_2 + O_2 \qquad \text{Equation (1)}$$

$$2H^+ + 2e^- \rightarrow H_2 \qquad \text{Equation (2)}$$

$$2H_2O + 4h^+ \rightarrow O_2 + 4H^+ \qquad \text{Equation (3)}$$

The mechanism of photocatalytic H_2O splitting along with the thermodynamic potential for the half reactions is shown in Figure 3. The presence of a co-catalyst in the CB of the catalysts is typically required to allow the protonation of H^+ to H_2. Common co-catalysts are highlighted in Figure 2 and include Pt (Yamaguti and Sato, 1984), RuO_2 (Inoue, 2009) and NiO (Hu and Teng, 2010).

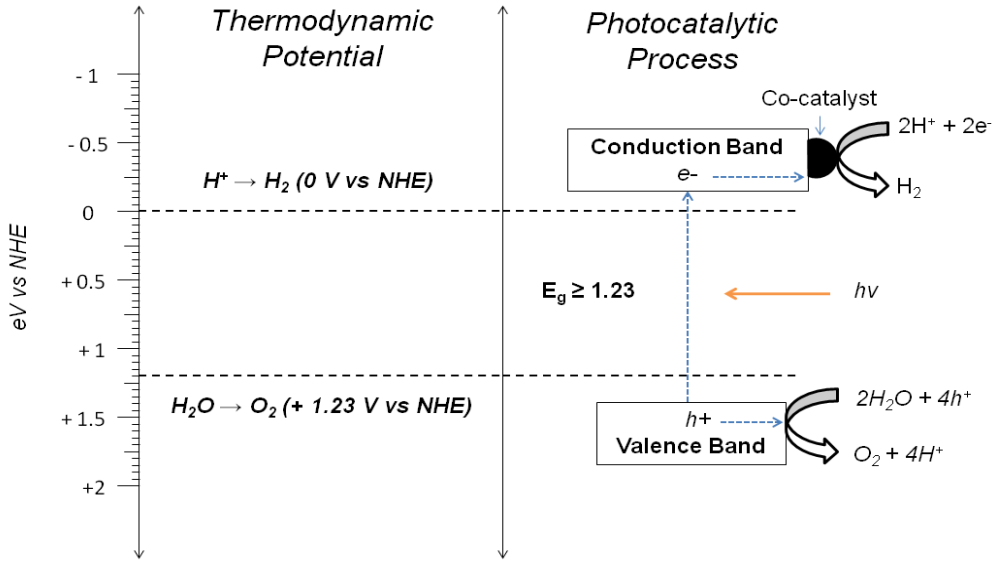

Figure 3; Mechanism of photocatalytic H_2O splitting

The band positions of common catalysts are shown in Figure 4 in relation to the required potential of H_2O splitting. The E_g of the catalysts are shown and as can be seen there are few catalysts which possess an E_g suitable for excitation by wavelengths in the visible region of the electromagnetic spectrum.

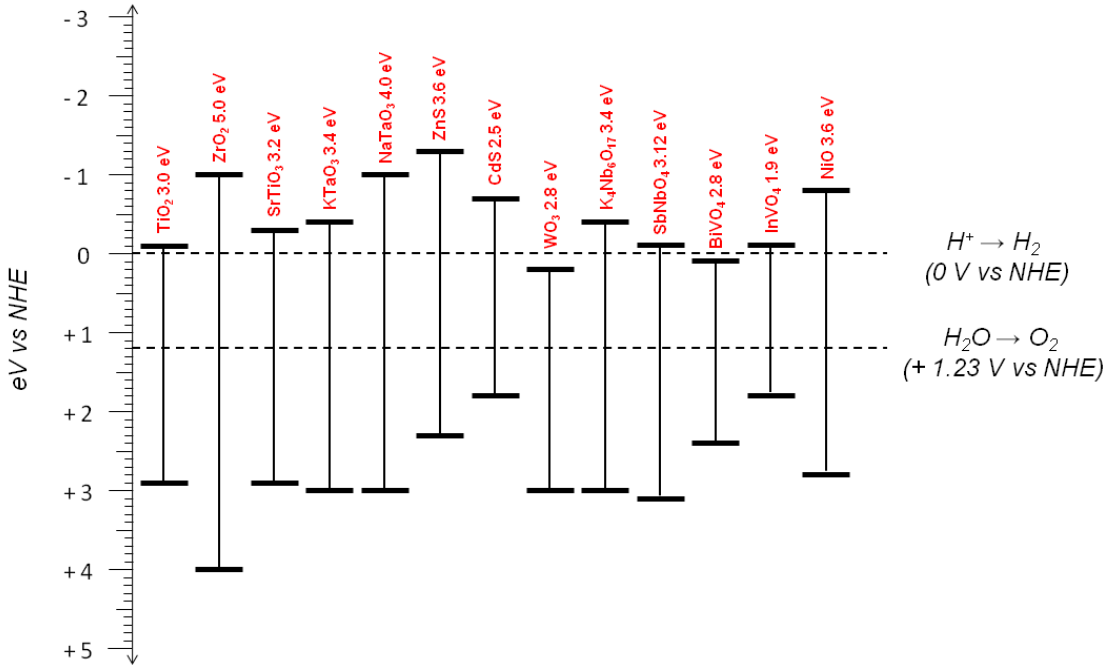

Figure 4; Band position of selected catalysts and the potential for H_2O splitting

The band position of the catalyst is not the sole requirement for H_2O splitting to proceed as a number of additional requirements must be addressed. Suppressing the recombination of holes and electrons along with efficient charge separation are key requirements. The creation and separation of active sites for H_2 and O_2 evolution is also important. It has been suggested that the separation of evolution sites should be on the nanometre scale to ensure the back reaction of O_2 and H_2 does not occur (Kato *et al.* 2003). Suppressing the back reaction will also prevent the formation of any intermediates in the process. The catalyst structure has been investigated to improve the catalytic activity through charge separation and back reaction suppression. A number of catalyst structures have been reported including anatase, perovskite, layered structure, tunnel structure and cubic pyrochlore. While these structures may differ in chemical composition and crystal phase, the presence of an MO_6/MO_4 (M = transition/typical metal) octahedral/tetrahedral unit is often present and has been reported to play a key role in the activity exhibited by a catalyst. Furthermore, the distortion of this fundamental unit as a result of the M-O-M bond angle has also been found to impact activity.

2.1 d^0 configuration catalysts

Transition metals with a vacant d orbital have shown activity towards H_2O decomposition with a range of catalysts reported (Kudo and Miseki 2009; Inoue 2009). The core metal ion of the catalysts reported include Ti^{4+}, Zr^{4+}, V^{5+}, Nb^{5+}, Ta^{5+} and W^{6+}. All of the metal ions have a d^0 electronic configuration. Discussed here are key examples of catalysts with a d^0 configuration based upon the core metal ion.

2.1.1 Titanates

Ti based catalysts have been extensively used in the field of photocatalysis, specifically the use of TiO_2. Photocatalytic splitting of water over TiO_2 was first reported by Fujishima and Honda using a photoelectrochemical system. The system comprised a TiO_2 electrode with Pt counter electrode, which used an external bias from a power supply. Upon UV illumination, electrons and holes were generated in the system which contributed to the reduction and oxidation of H_2O. On the Pt counter electrode the electrons reduced H_2O to H_2, while H_2O was oxidised to O_2 on the TiO_2 electrode. In contrast to this, powdered TiO_2 catalysts are not capable of splitting water without modification to the catalyst such as the addition of a co-catalyst.

In the early stages of water splitting research the capability of Pt-loaded TiO_2 was questionable due to low yields of products and no O_2 evolution. A number of publications, however showed the evolution of both H_2 and O_2 over platinised TiO_2 using NaOH coatings (Yamaguti and Sato, 1984; Yamaguti and Sato 1985) and the addition of alkali carbonates (Sayama and Arakawa, 1997). Yamaguti and Sato found that a 10 wt % NaOH coating onto Pt-TiO_2 to be effective for H_2O splitting, producing a quantum yield of 17 %. Following their study in 1984, Sayama and Arakawa (1985) further increased the quantum yield to 29 % when using a NaOH coated Rh-TiO_2 catalyst. The enhanced activity of Pt-TiO_2 was due to the ability of Pt to restrict the recombination of electrons and holes and catalyse proton reduction (Zheng *et al.* 2009; Yang *et al.* 2012; Mizukoshi *et al.* 2007). Pt has improved electron acceptor properties as a result of a larger work function (5.65 eV), as described by Mizukoshi *et al.* (2007), which prevents the recombination of photo generated electrons and holes.

The addition of carbonate salts to a Pt-TiO_2 suspension was shown to increase the production of H_2 and O_2 from H_2O splitting. Sayama and Arakawa (1997) found Pt-TiO_2 in suspension with 2.2 M Na_2CO_3 produced 568 μmol h^{-1} and 287 μmol h^{-1} of H_2 and O_2 respectively, which conforms to the stoichiometric ratio of 2:1. The presence of carbonate species on the Pt-TiO_2 catalyst played a significant role in the reaction pathway. On the Pt, absorbed carbonates suppressed the H_2O splitting back reaction while on TiO_2, the effective desorption of O_2 prevented photoadsorption.

The use of layered perovskites catalysts has been reported in literature using a range of titanates including $Rb_2La_2Ti_3O_{10}$ (Takata *et al.* 1997), $KaLaZr_{0.3}Ti_{0.7}O_4$ (Reddy *et al.* 2003), $KTiNbO_5$ (Takahashi *et al.* 1999), $SrTiO_3$ (Domen *et al.* 1986), $K_2La_2Ti_3O_{10}$ (Haung *et al.* 2008), $La_2Ti_2O_7$ (Kim *et al.* 1999), $La_4CaTi_5O_{17}$ (Kim *et al.* 1999), $Gd_2Ti_2O_7$ (Abe *et al.* 2006) and $Y_2Ti_2O_7$ (Abe *et al.* 2006). The activity exhibited by such layered structure catalysts is a result of the interlayer space formed resulting in the increased presence of evolution sites. Additionally, the evolution sites in a layered structure are sufficiently separated from one another to suppress the back reaction of H_2 and O_2. The catalyst $LaCaTi_5O_{17}$, which had a 110 layered perovskite structure, was reported by Kim and colleagues in 1999 to generate a high quantum yield of 20 % under UV irradiation at < 320 nm. Takata *et al.* (1997) reported evolution rates of 444 and 221 μmol h^{-1} for H_2 and O_2 respectively over Ni-$K_2La_2Ti_3O_{10}$, while Ikeada *et al.* (2006) later reported increased rates of 2186 and 1131 μmol h^{-1} for H_2 and O_2 respectively over the same catalyst synthesised by a polymerised complex method. The structure of $K_2La_2TiO_{10}$ and $K_2La_2Ti_3O_{10}$ with a hydrated layer is shown in Figure 5. The structure consists of negatively charged titanoanthanate perovskite layers and interlayer K^+ ions.

(a)

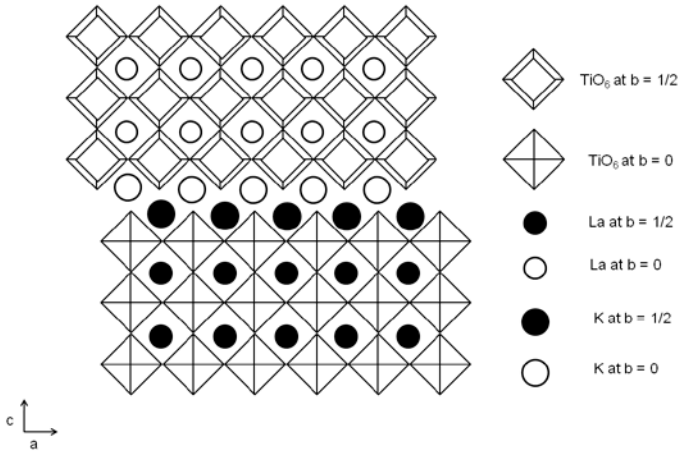

(b)

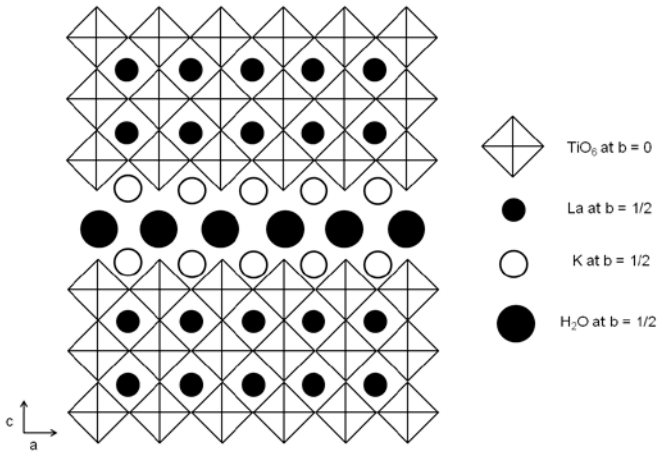

Figure 5; Structure of (a) $K_2La_2Ti_2O_{10}$ and (b) $K_2La_2Ti_2O_{10}.H_2O$ (reproduced from Huang *et al*. (2008), with kind permission of Elsevier)

Abe *et al*. (2006) also showed that catalysts with a perovskite structure were active for H_2O splitting, however, demonstrated for the first time that titanates with a pyrochlore structure were also active, Figure 6. The cubic pyrochlore catalysts Y_2TiO_7 (3.5 eV) and Gd_2TiO_7 (3.5 eV) along with the monoclinic perovskite $La_2Ti_2O_7$ (3.8 eV) were capable of evolving both H_2 and O_2 from distilled water under irradiation from a 400 W Hg lamp. The catalysts were loaded with NiO to split pure H_2O into H_2 in the range of 307 - 850 μmol h^{-1} and O_2 in the range of 152 - 420 μmol h^{-1}. Abe and colleagues found that the activity of $Y_2Ti_2O_2$, $Gd_2Ti_2O_7$ and $La_2Ti_2O_7$ was dictated by the crystal structure of the catalyst. The authors reported that the cubic pyrochlore structure of $Y_2Ti_2O_7$ and $Gd_2Ti_2O_7$ and the monoclinic perovskite structure of $La_2Ti_2O_7$ both possessed a network of corner-shared octahedral units of the metal cation TiO_6. The presence of the corner units allows the formation of networks which are capable of increasing the mobility of charged particles. The study also showed that catalysts without this structure showed minimal activity, indicating the dependency of crystal structure on H_2O splitting.

(a) (b)

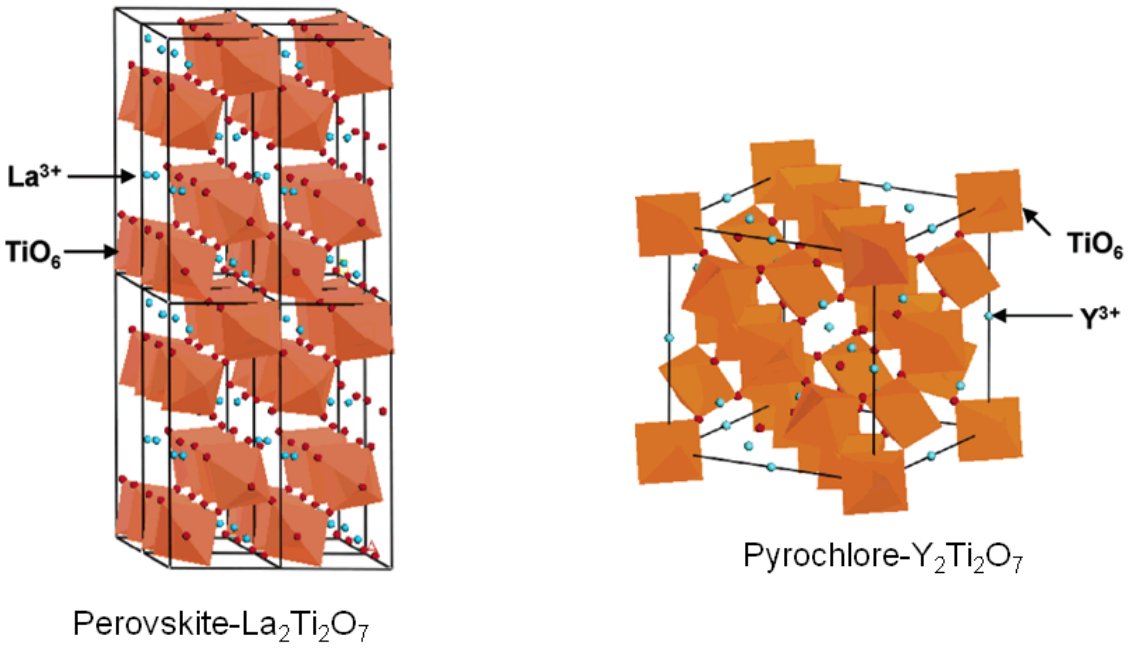

Figure 6; Structure of (a) $La_2Ti_2O_7$ and (b) $Y_2Ti_2O_7$ (reproduced from Abe *et al.* (2006), with kind permission of American Chemical Society)

The engineering of catalyst structures for H_2O splitting can play a key role in developing an efficient compound. The development of nanotubes arrays (Yang *et al.* 2012; Altomare *et al.* 2013) along with TiO_2 thin films (Kitano *et al.* 2007) has been reported. Kitano and colleagues reported a visible light responsive system using a Pt-TiO_2 thin film to generate H_2 and O_2 from methanol and silver nitrate solutions respectively. Nanotube structures reported by Yang and colleagues used a Nb doped $TiO_2/SrTiO_3$ catalyst in their photoelectrochemical studies, while Altomare *et al.* developed a system which consisted of TiO_2 nanotubes grown on a Ti support, Figure 7. The Altomare *et al.* system yielded separate evolution streams of H_2 and O_2 without any electrical bias or sacrificial agent. An electrochemical anodisation method was used to synthesise self-organised nanotube arrays. The activity of the system was reported in terms of H_2 and O_2 evolution rates at 80 and 43 μmol h^{-1} respectively. Based upon the production of H_2 a quantum yield of 15 % was also reported under optimum conditions. This approach to H_2O splitting has numerous advantages over the use of more traditional catalysts for the decomposition of H_2O with a view towards clean H_2 production. There are a number of limitations which can restrict the large scale applicability of powdered systems including fast rates of recombination, recovery from aqueous reaction solutions and down stream processing

techniques associated with H_2 and O_2 separation from a mixture. Deploying a nanotube array system can suppress these limitations to construct a method of attaining high purity H_2.

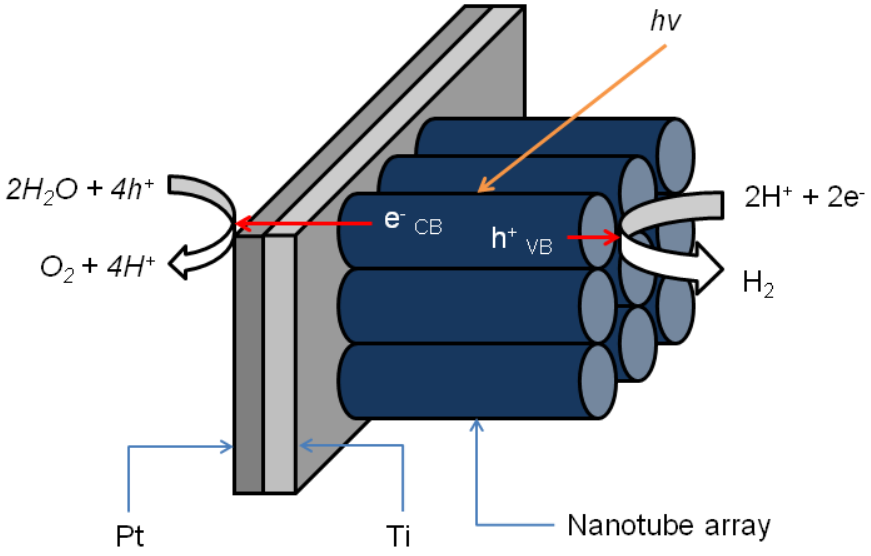

Figure 7; Schematic of nanotube array on a titania support with a Pt electrode (reproduced from Altomare *et al.* (2013), with kind permission of Elsevier)

2.1.2 Tantalates

The use of tantalate based catalysts has been used extensively in the field of photocatalytic H_2O splitting. Alkali and alkaline earth tantalates have exhibited high activity towards H_2O splitting to H_2 and O_2 in stoichiometric quantities. A number of Ta based complexes have been studied including $K_3Ta_3Si_2O_{13}$, $ATaO_3$ (A = Li, Na, K), $Sr_2Ta_2O_7$, $RbLnTa_2O_7$, $K_2LnTa_5O_{15}$ and $A_2SrTa_2O_7.nH_2O$ (A = H, K, Rb). While these compounds vary in chemical composition and crystal structure they all posses a TaO_6 octahedral interconnected in the 1-, 2- or 3-D manner. As discussed previously with Ti based catalysts, the presence of a corner metal cation in the structure of catalysts has proven to be key for efficient H_2O splitting to proceed. In particular the distortion of this structure has been found to further increase activity through increased charge separation (Kim *et al.* 2012). The distortion of the catalyst structure is dictated by the angle of the M-O-M bond, where generally an angle of $< 180^{o}$ results in distortion.

The presence of a TaO_6 corner unit has been reported to be present in catalysts with a pyrochlore, (layered) perovskite and weberite structure. This fundamental unit has been reported to contribute to the formation of the CB, which was shown recently in work by Kim *et al.* (2012) who developed

niobate and tantalate layered crystal catalysts with ferroelectric properties. Catalysts $SbNbO_4$ (3.12 eV) and $SbTaO_4$ (3.7 eV) were synthesised using a conventional solid-state reaction method. The increased E_g of $SbTaO_4$ was found to be a result of the distortion of the crystal structure, which was dictated by the angle of the Ta-O-Ta bond (130 ^{o}) in the TaO_6 octahedral. In contrast the 150 ^{o} angle of Nb-O-Nb bonds in $SbNbO_4$ resulted in the compound being distortion free. Kato and Kudo also reported that a decrease in the Ta-O-Ta bond angle from 180 ^{o} to 143 ^{o} in their catalysts $KaTaO_3$ and $LiTaO_3$ resulted in distortion (Kato and Kudo, 2003). These observations by Kim *et al.* and Kato and Kudo were found to impact photocatalytic activity. Under optimum conditions 2.4 μmol h^{-1} and 5.8 μmol h^{-1} H_2 was evolved over $SbNbO_4$ and $SbTaO_4$ respectively. The authors hypothesised that the 58.6 % increase in H_2 production over $SbTaO_4$ was a result of the increased CB band edge of Ta 5d orbitals in the TaO_6 octahedral along with efficient charge separation due to the dielectric constant which was induced by the distorted crystal structure of the $SbTaO_4$ catalyst.

While the presence of a MO_6 metal octahedral structure has been shown to be significant, it is the metal at the M position which is also essential for photocatalytic activity. In 2006 Abe *et al.* showed that the level of distortion of the catalyst La_3TaO_7 and the presence of TaO_6 octahedral corner units increased H_2O splitting activity. The distortion of the crystal structure was a result of the ionic radius of rare earth metals in R_3TaO_7 (R = rare earth metal). The distortion caused a change in structure from cubic fluorite to cubic pyrochlore and then to orthorhombic weberite. Despite pyrochlore structured catalysts previously being reported active by Ikeada *et al.* (2006), negligible activity was found when the cubic fluorite and pyrochlore catalysts were deployed. In contrast, the webertie structure catalyst showed significant H_2O splitting; 164 μmol h^{-1} H_2 and 80 μmol h^{-1} O_2.

The activity of La_3TaO_7 for H_2O splitting was found to increase with the shift in crystal structure from cubic pyrochlore to orthorhombic weberite. The weberite structure was composed of zig-zag chains formed by corner-shared TaO_6 octahedrons, as shown in Figure 8 (a). While it was found that the catalysts with a cubic pyrochlore (Gd_3TaO_7/La_3TaO_7) structure did contain TaO_6 units, the structure also revealed the presence of GdO_6 and LaO_6 corner units, Figure 8 (b). The ratio of TaO_6 and Gd/LaO_6 units was in a ratio of 1:1. It was found that the network of octahedrons increases the mobility of the charged particles (electrons and holes) in the catalyst structure. Work conducted by Zheng and West (1991) showed that the weberite structure of La_3TaO_7 exhibited high electrochemical conductivity. This conductivity can increase the mobility of charged particles, which can increase the probability of electrons and holes reaching an active site located on a catalyst surface.

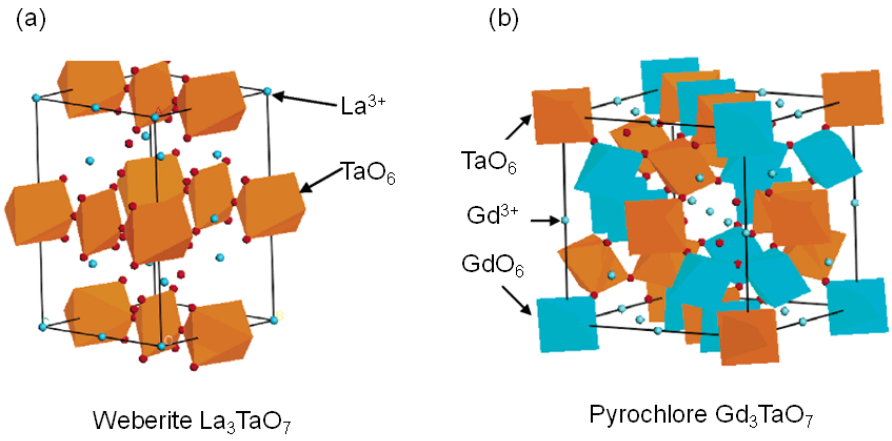

Figure 8; Structure of orthorhombic weberite La_3TaO_7 and pyrochlore Gd_3TaO_7 (reproduced from Abe *et al.* (2006), with kind permission of American Chemical Society)

The use of the catalyst $NaTaO_3$, with a distorted perovskite structure, has received an increased level of attention due to the high quantum yields reported (Kato and Kudo 2003; Kato *et al.* 2003; Kudo and Kato, 2000). As discussed earlier in the chapter, displaying catalyst activity as quantum yield is key to understanding the efficiency of the compound in relation to the quantity of photons absorbed and products evolved. The activity of this catalyst has been significantly improved by the addition of co-catalysts and doping of lanthanides. Kudo and Kato (2000) investigated the production of H_2 and O_2 over $NaTaO_3$ catalysts doped with a range of lanthanides. The E_g of the catalysts synthesises ranged from 4.01 – 4.09 eV, which limited them to UV excitation by a 400 W high-pressure Hg lamp. All catalysts deployed displayed activity towards H_2 and O_2 evolution from distilled H_2O in the conventional ratio of 2:1. The highest activity recorded was over $NaTaO_3$:La using NiO as a co-catalyst at 5.9 μmol h^{-1} and 2.6 μmol h^{-1} for H_2 and O_2 respectively. This rate of production produced an AQY of ~50 % at 270 nm. Kato and Kudo further reported an AQY of 50 % at 270 nm in 2003 along with a discussion into the crystal structure of the catalyst. Later in 2003, Kato *et al.* reported the highest apparent quantum yield for the catalyst at 56 % at 270 nm. The optimum conditions were a La doped loading of 2 mol % and NiO loading of 0.2 wt %, which produced 19.8 μmol h^{-1} and 9.66 μmol h^{-1} H_2 and O_2 respectively. The activity of this catalyst was found to be due to the structure of the catalyst which consisted of a TaO_6 corner unit, as previously discussed. The authors, however, also discussed the importance of the nanostep structure in H_2O splitting. The authors used transmission electron microscope and extended X-ray absorption fine structure analysis to conclude that H_2 evolution occurred on the ultrafine NiO particles, which were loaded onto the nanostep structure of the catalyst while O_2 proceeded at the groove of the nanostep structure.

2.1.3 Niobates

As has previously been discussed the activity of niobate catalysts and the structure of the compound are closely linked. Common structures which have been reported in Nb based catalysts include layered perovskites, pyrochlores and wolframite (Zou *et al.* 2003). The initial research into complexes with a layered structure was primarily conducted using Nb based catalysts. A number of Nb catalysts, with a layered structure, have been reported active for H_2O splitting including $A_{2.23}Sr_{0.67}Nb_5O_{14.335}$ (A = K, H) (Li *et al.* 2009), In-$H_2LaNb_2O_7$ (Wei *et al.* 2009), NiO-K_4NbO_{17} (Lin *et al.* 2008), Pt-K_4NbO_{17} (Sayama *et al.* 1998), $K_{0.5}La_{0.5}Bi_2Nb_2O_9$ (Chen *et al.* 2012), $SbNbO_4$ (Kim *et al.* 2012), $Sr_2(Ta_{1-x}Nb_x)_2O_7$ (Kato and Kudo, 2001) and Ni-$A_4Ta_xNb_{6-x}O_{17}$ (A = K, Rb) (Sayama *et al.* 1996). The structured catalysts have been shown to have two interlayer spaces (interlayers I and II) present, the advantages of which were discussed in Section 2.1.1. Co-catalysts were found to be present in the interlayers; Domen *et al.* (1986) impregnated NiO into $K_4Nb_6O_{17}$, Sayama *et al.* (1998), Li *et al.* (2009) and Wei *et al.* (2009) all interlaced Pt into $K_4Nb_6O_{17}$, $A_{2.33}Sr_{0.67}Nb_{514.335}$ (A = K, H) and In-$H_2LaNb_2O_7$ respectively.

The publication by Domen and colleagues in 1986 was one of the earliest reports of the layered compound $K_4Nb_6O_{17}$ (3.3 eV) being used for H_2O splitting. Since the initial publication, $K_4Nb_6O_{17}$ and its variations have been reported frequently. While Domen *et al.* reported that stoichiometric evolution of H_2 and O_2 was achieved over bare $K_4Nb_6O_{17}$, an 1 order of magnitude increase was reported when using NiO as a co-catalyst. Under favourable conditions a maximum quantity of 80 μmol h^{-1} H_2 and 38 μmol h^{-1} O_2 was recorded.

Sayama and colleagues reported the synthesis of $K_4Nb_6O_{17}$ by photoreduction and H_2 reduction methods. Under photoreduction synthesis the Pt particles were found to be < 6 Å, which allowed the fine particles to occupy interlayer I, Figure 9. Under the H_2 reduction method particles were found to be > 15 Å, which were too large to occupy the interlayer space and resulted in the destruction of the catalyst layers. The results of the research showed the photoreduction synthesised catalyst to have higher activity than the H_2 reduction catalyst. In a suspension of Na_2CO_3 451 μmol h^{-1} and 217 μmol h^{-1} H_2 and O_2 were produced respectively over Pt-$K_4Nb_6O_{17}$ by photoreduction, while over Pt-$K_4Nb_6O_{17}$ by H_2 reduction 293 μmol h^{-1} and 123 μmol h^{-1} H_2 and O_2 were produced respectively. The authors found that O_2 production occurred within interlayer II, while H_2 production proceeded in interlayer I with the addition of carbonate anions suppressing the back reaction of H_2 and O_2 over Pt.

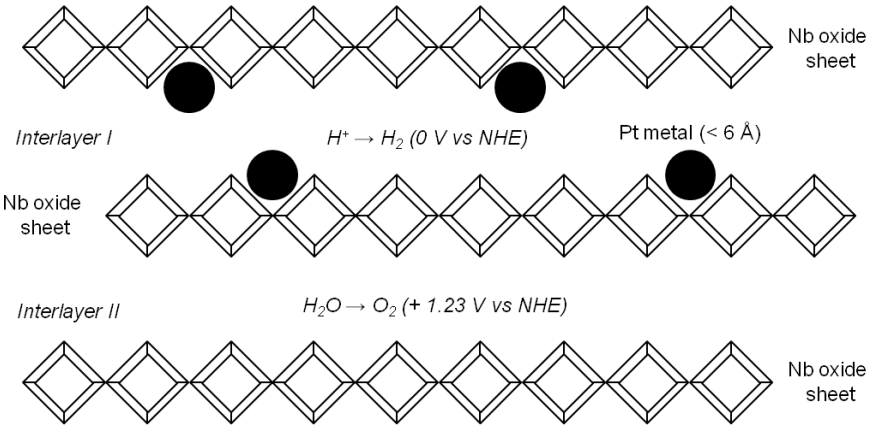

Figure 9; Structure of interlayers in Pt-$K_4Nb_6O_{17}$ (reproduced from Sayama *et al*. (1998), with kind permission of Elsevier)

In 1996, Sayama *et al.* found that $Rb_4Nb_6O_{17}$ also exhibited H_2O splitting activity. The research group observed an increase from 403 μmol h^{-1} H_2 and 197 μmol h^{-1} O_2 to 936 μmol h^{-1} H_2 and 451 μmol h^{-1} O_2 over Ni-$K_4Nb_6O_{17}$ and Ni-$Rb_4Nb_6O_{17}$ respectively. A series of catalysts were developed by Sayama and colleagues which comprised of Ni-$A_4Ta_xNb_{6-x}O_{17}$, where A = K or Rb. The highest activity was observed when x = 0 with a decreasing trend seen when the substitution of Nb for Ta increased. When x = 6, Ta was fully substituted for Nb and a significantly low level of H_2/O_2 was evolved; 11 μmol h^{-1} H_2 and 1 μmol h^{-1} O_2. The decrease in evolution was primarily a result of the difference in E_g of Ni-$Rb_4Ta_6O_{17}$ (4.1 eV) and Ni-$Rb_4Nb_6O_{17}$ (3.5 eV). Despite the difference in E_g, the quantum yields of the catalysts were similar, which was a result of $Rb_4Ta_6O_{17}$ absorbing less photons than $Rb_4Nb_6O_{17}$.

In 2003 a series of different structural Nb catalysts were investigated including an $A_2B_2O_7$ cubic pyrochlore, ABO_4 wolframite and ABO_4 stibotantalite type structures with a view towards visible light H_2O splitting (Zou *et al.* 2003). As has been discussed in this chapter, despite the catalysts varying in crystal structure they were all found to posses octahedral NbO_6 units. The layered wolframite structure was shown to contain both NbO_6 and InO_6 octahedral corner sharing units, which contributed to the formation of the structure. The NbO_6 units formed zig-zag chains of [NbO_3], which were connected through the InO_6 units to form the network, Figure 10. The E_g of $InNbO_4$ was calculated at 2.5 eV, which was suitable for absorption of visible wavelengths. Under irradiation from a 300 W Xe lamp with a 420 nm cut off filter the evolution of H_2 from pure H_2O was observed over NiO-$InNbO_4$. Under these experimental conditions, it should be noted that O_2 evolution was not recorded, with the authors suggesting any O_2 evolved was photoabsorbed onto the catalysts structure.

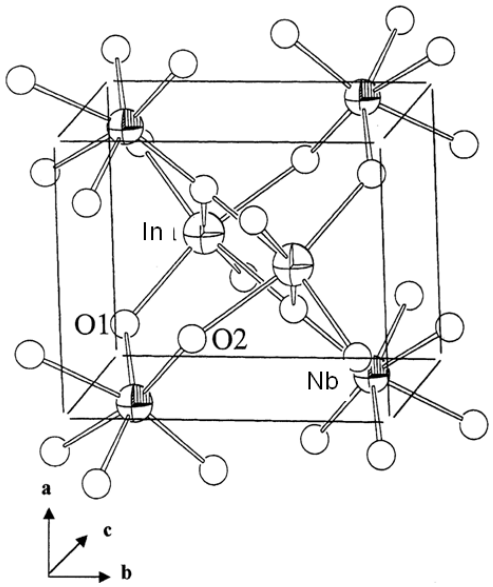

Figure 10; Schematic structure of $InNbO_4$ (reproduced from Zou *et al*. (2003), with kind permission of International Association of Hydrogen Energy)

2.1.4 Vanadates and Tungstanates

A number of additional transition metal oxides have been reported to be active for H_2O splitting including ZrO_2 (Reddy *et al.* 2003), $PbWO_4$ (Kadowaki *et al.* 2007), $BiVO_4$ (Hau Ng *et al.* 2010), Cu_2O (Hara *et al.* 1998), $InVO_4$ (Ye *et al.* 2002) and Sr-CeO_2 (Kadowaki *et al.* 2007).

The use of vanadium oxide (VO_4) catalysts for H_2O splitting is of particular interest due to the activity reported under visible light irradiation (Ye *et al.* 2002; Hau Ng *et al.* 2010). Hau Ng and colleagues used $BiVO_4$ in conjunction with reduced graphene oxide (RGO) in a photoelectrochemical system to generate H_2 and O_2, Figure 11, while $InVO_4$ was deployed by Ye *et al.* Over RGO-$BiVO_4$, production rates of 0.75 and 0.21 μmol h^{-1} were achieved for H_2 and O_2 respectively, which was a 4.2 % increase over pure $BiVO_4$. The improvement in activity was a result of photoexcited electrons injecting into the RGO, thus prolonging the lifetime and suppressing recombination. The rate of transition of the photoelectron to the Pt counter electrode was significantly faster using RGO over pure $BiVO_4$.

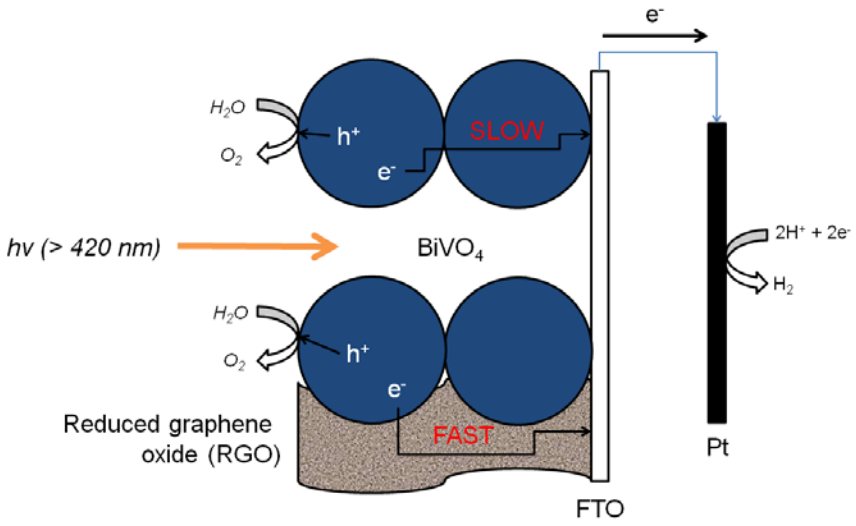

Figure 11; Schematic representation of H_2O splitting mechanism on RGO-$BiVO_4$ (reproduced from Hau Ng *et al.* (2010), with kind permission of American Chemical Society)

The activity of NiO-$InVO_4$ was reported in relation to H_2 production under irradiation from a 300 W Xe arc lamp using a 420 nm cut-off filter. The E_g of the catalyst was calculated at 1.9 eV which was formed from the V 4d orbital in VO_4. The structure of the catalyst was found to consist of both InO_6 octahedral units and VO_4 tetrahedral units, which was similar to that reported for $InNbO_6$ (Zou *et al.* 2003). The production rate of H_2 from pure water was ~3.25 μmol h^{-1} over $InVO_4$ with a 1.0 wt. % loading of NiO. There was no evolution of O_2, which the authors hypothesised was due to O_2 photoabsorbing onto the catalyst surface in a physisorbed and /or chemisorbed molecular state (Ye *et al.* 2002).

2.2 d^{10} configuration catalysts

2.2.1 d^{10} metal oxides

The observation was made by Inoue in 2009 that since metal oxides with a vacant d orbital (d) are efficient photocatalysts, metal oxides with a filled d orbital will also be efficient. It has been reported that catalysts constructed using In^{3+}, Ga^{3+}, Ge^{4+}, Sn^{4+} and Sb^{5+} along with RuO_2 as a co catalyst, exhibit photocatalytic H_2O splitting activity. Work conducted primarily by Inoue's research group has highlighted the potential of d^{10} metal oxides for water splitting. A number of key catalysts were reviewed by Inoue (2009) including layered catalysts such as $NaInO_2$ and $CaSb_2O_6$, weberite catalysts $Ca_2Sb_2O_7$ and $Sr_2Sb_2O_7$ and willemite catalyst Zn_2GeO_4. Inoue (2009) and Kudo and Miseki (2009) both discussed the importance of RuO_2 as a co-catalyst for d^{10} for metal oxides. In the absence of RuO_2 the catalysts exhibited minimal activity. An exception was the catalyst Ga_2O_3,

which previously displayed activity when loaded with NiO. The catalyst, with an E_g of 4.6 eV, produced 46 μmol h^{-1} H_2 and 23 μmol h^{-1} O_2. Using Ni as a co-catalyst, a Zn doped Ga_2O_3 was found to be highly active (Sakata *et al.* 2008). Using irradiation form 450 W Hg lamp 4100 μmol h^{-1} H_2 and 2200 μmol h^{-1} O_2 was evolved.

The distortion of catalyst structure in a series of compounds researched by Inoue's group has been published. Catalysts investigated included alkaline earth metal MGa_2O_4 (M = Mg, Ca, Sr), $MSnO_4$ (M = Ca, Sr, Ba), $NaSbO_3$, $CaSb_2O_6$ and $M_2Sb_2O_7$ (M = Ca, Sr) (Inoue, 2009; Sato *et al.* 2002). In 2002 Sato and colleagues found 1 wt. % RuO_2 loaded $Sr_2Sb_2O_7$ to exhibit the highest level of activity over other antimonate catalysts due to its weberite structure consisting of two distorted SbO_6 units. The compression and elongation of Sb-O bonds gave rise to the distorted octahedral shapes shown in Figure 12.

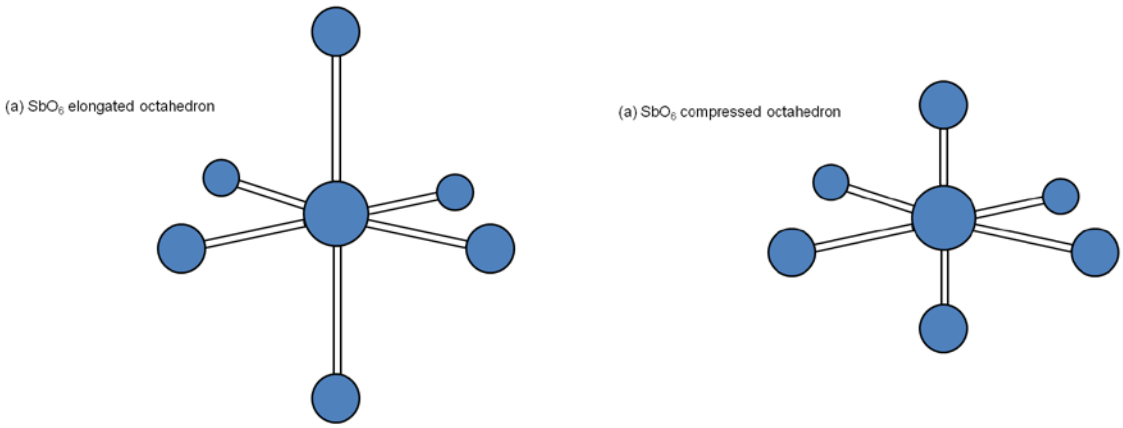

Figure 12; Structure of (a) SbO_6 elongated and (b) SbO_6 compressed octahedron

The structures of MGa_2O_4 (M = Mg, Ba, Sr) were found to be cubic with a GaO_6 octahedron when M = Mg, monoclinic with a GaO_4 tetrahedron when M = Sr and hexagonal with a GaO_4 tetrahedron when M = Ba. The activity of these compounds was investigated in relation to their dipole moments, which were calculated to be 0 D for $MgGa_2O_4$, 0.80 and 1.2 D for $SrGa_2O_4$ and 1.70, 1.11 and 2.58 D for $BaGa_2O_4$. The dipole moment, which is a measure of difference in electronegativity, indicates the level of distortion in a compound. $MgGa_2O_4$ had a dipole moment of 0 which suggested the catalyst was distortion free, while $SrGa_2O_4$ and $BaGa_2O_4$ both had increased dipole moments suggesting they had a distorted structure. The authors found that the distorted structure of $SrGa_2O_4$ and $BaGa_2O_4$ were photoactive while the distortion free structure of $MgGa_2O_4$ was not. A similar observation regarding distorted structures was made when using stannates doped with Ca, Sr and Ba. Ca_2SnO_4

and Sr_2SnO_4 were found to exhibit photocatalytic H_2O splitting activity, while Ba_2SnO_4 displayed negligible results. The fundamental unit, SnO_6, in the crystal structure of Ca_2SnO_4 and Sr_2SnO_4 was found to be distorted while in Ba_2SnO_4 it remained distortion free.

The activity exhibited by catalysts with a distorted structure is interesting and a number of possible explanations have been reported. Inoue (2009) suggested that the length of metal-oxygen bonds impacts photoexcitation. The poor symmetry formed as a result of distorted octahedral and tetrahedral structures results in isolated orbitals, which gives rise to different photoexcitation efficiencies. Inoue also suggested that the local internal fields of the compounds as result of the dipole moment could increase electron-hole separation and suppress recombination.

2.2.2 d^{10} metal nitrides

The investigation of metal nitrides (and oxynitrides) is an interesting area of H_2O splitting research and publications in this field are increasing. The advantage of metal nitrides and oxynitrides is the potential of synthesising visible light responsive photocatalysts for overall H_2O splitting. The VB of metal nitrides is composed of N2p, which has a higher energy level than that of O2p in metal oxides. Therefore the E_g is narrower, presuming the CB remains the same, which allows for excitation by photons with a wavelength > 400 nm. A number of d^0 transition metal oxides have been investigated such as Ta_3N_5 (Hitoki *et al.* 2002), TaON (Hitoki *et al.* 2002), $MTaO_2N$ (M = Ca, Sr, Ba) (Yamasita *et al.* 2004) and $LaTiO_2N$ (Kasahara *et al.* 2002), however minimal activity was reported. Metal nitrides with a d^{10} configuration, however, have the advantage of forming large band dispersion at the CB, which yields highly mobile photoexcited electrons (Inoue, 2009; Moriya *et al.* 2013).

Examples of metal nitrides being used include β-Ge_3N_4 (Maeda *et al.* 2006), doped GaN and GaN in a solid solution with ZnO (Maeda *et al.* 2005; Maeda *et al.* 2006; Yoshida *et al.* 2013; Lee *et al.* 2012). These catalysts have all shown activity towards H_2O splitting when used with RuO_2 as a co-catalyst. RuO_2-β-Ge_3N_4 was the first successful example of a non metal oxide catalyst being deployed for overall H_2O splitting (Inoue, 2009).

The activity of $(Ga_{1-x}Zn)(N_{1-x}O_x)$, synthesised from Ga_2O_3 and ZnO, has been reported by a number of research groups (Maeda et al, 2005; Maeda *et al.* 2006; Lee *et al.* 2012; Yoshida *et al.* 2013). The interest in this catalyst has grown due to its high level of activity and potential for visible light activation. Maeda *et al.* (2005) reported their samples of $(Ga_{1-x}Zn)(N_{1-x}O_x)$ to have an E_g in the range of 2.6 - 2.8 eV, which is lower than that of the individual catalysts ZnO (3.2 eV) and GaN (3.4 eV) and suitably low enough to permit excitation by absorbed visible photons. More recently, Lee *et al.* (2012) have further minimised the E_g to 2.2 eV by increasing x to 0.87, which they concluded can significantly increase the absorption of solar photons. Using a 5 wt % of RuO_2, Maeda and colleagues

(2005) found the catalyst was active under UV and visible illumination, producing stoichiometric quantities of H_2 and O_2. The highest activity was reported over $(Ga_{1-x}Zn)(N_{1-x}O_x)$ where x = 0.12 and the nitridation time was 15 hr. The authors found that the longest wavelength available for water splitting was 460 nm, which corresponded to the absorption edges of the catalyst. Following this publication Maeda and colleagues published an additional paper in 2006 reporting an increased activity of $(Ga_{1-x}Zn)(N_{1-x}O_x)$ doped with Cr and a series of transition metals under UV irradiation. Using 1 wt % Rh and 1.5 wt % Cr, 3835 μmol h^{-1} H_2 and 1988 μmol h^{-1} O_2 was evolved over $(Ga_{1-x}Zn)(N_{1-x}O_x)$ from distilled water.

Recently it was reported that the activity of the Rh doped $(Ga_{1-x}Zn)(N_{1-x}O_x)$ catalyst under visible irradiation was further increased using lanthanoid oxide layers (Yoshida *et al.* 2013). Using a 300 W lamp with a cut off filter (> 400 nm), H_2 and O_2 was evolved over Rh-$(Ga_{1-x}Zn)(N_{1-x}O_x)$ catalysts doped with La, Pr, Sm, Gd and Dy, while un doped Rh-$(Ga_{1-x}Zn)(N_{1-x}O_x)$ displayed no activity. It was found the presence of lanthanoid oxide layers act as Rh modifiers and suppress the back reaction of H_2 and O_2 over Rh.

Electronic Configuration	Core Metal Ion	Catalyst	Co-catalyst	E_g	Reaction solution	Activity (μmol h^{-1})		AQY (%)	Reference
						H_2	O_2		
d^0	Ti^{4+}	TiO_2	Pt	3.2	H_2O/ 2.2 M Na_2CO_3	568	287		Sayama and Arakawa (1997)
		TiO_2	Rh	3.2	3 M NaOH	449	-	29	Yamaguti and Sato (1985)
		$Sr_3Ti_2O_7$	NiO	3.2	Pure water	83	42	4.3	Jeong *et al.* (2006)
		$K_2La_2Ti_3O_{10}$	NiO	3.5	H_20/ 0.1 M KOH	444	221		Takata *et al.* (1997)
		$Na_2Ti_6O_{13}$	RuO_2	-	Pure water	~17	~8		Ogura *et al.* (1998)
		$BaTi_4O_9$	RuO_2	-	Pure water	~18	~8		Inoue *et al.* (1992)
	Zr^{4+}	ZrO_2	-	3.93	H_2O/ Na_2CO_3	88.8	45		Reddy *et al.* 2003
	V^{5+}	$InVO_4$	NiO	1.8	Pure water	69.1	34.5		Lin *et al.* (2008)
	Nb^{5+}	$K_4Nb_6O_{17}$	Pt	3.4	H_2O/ 2.2 M Na_2CO_3	451	217		Sayama *et al.* (1998)
		$SbNbO_4$	RuO_2	3.1	Pure water	~2.4	-		Kim *et al.* (2012)
		$H_{1.6}K_{0.2}La_{0.3}Bi_{0.1}Nb_2O_{6.5}$	-	3.49	Pure water	27.2	Trace		Chen *et al.* (2012)
	Ta^{5+}	NaTaO3:La	NiO	4.0	Pure water	19.8	9.66	56	Kato *et al.* (2003)
		$Sr_2Ta_2O_7$	NiO	4.55	Pure water	1000	500		Kato and Kudo (2001)
		$SbTaO_4$	RuO_2	3.7	Pure water	~5.8			Kim *et al.* (2012)
		$K_2Ta_2O_6$	NiO	4.6	H_2O/ NaOH	437	226		Ikeda *et al.* (2006)
	W^{6+}	$PbWO_4$	RuO_2	3.24	Pure water	~18	~8		Kadowaki *et al.* (2007)
d^{10}	Ga^{3+}	Ga_2O_3	NiO	4.6	Pure water	46	23		Inoue (2009)
		Ga_2O_3:Zn	Ni	4.6	Pure water	4100	2200		Sakata *et al.* (2008)
		GaN:ZnO	RuO_2	2.58	H_2O/ H_2SO_4	0.98	0.48	0.14	Maeda *et al.* (2005)
		$(Ga_{1-x}Zn)(N_{1-x}O_x)$	RuO_2	2.7	Pure water	3835	1988		Maeda *et al.* (2006)
	In^{3+}	$NaInO_2$	RuO_2	3.9	Pure water	0.9	0.3		Kudo and Miseki (2009)
		$SrIn_2O_4$	RuO_2	3.6	Pure water	7	3		Kudo and Miseki (2009)
	Ge^{4+}	β-Ge_3N_4	RuO_2	3.85	Pure water	0.8	0.4	9	Maeda *et al.* (2006)
	Sn^{4+}	Sr_2SnO_4	RuO_2	-	Pure water	5	2.5		Inoue (2009)
	Sb^{5+}	$Ca_2Sb_2O_7$	RuO_2	3.6	Pure water	2.9	1		Sato *et al.* (2002)
		$Sr_2Sb_2O_7$	RuO_2	4.0	Pure water	8	3		Sato *et al.* (2002)
		$NaSbO_3$	RuO_2	3.6	Pure water	1.7	0.8		Sato *et al.* (2002)

Table 1; Overview of selected publications for overall water splitting

2.3 Z-scheme photocatalysts

The use of a single visible light responsive photocatalyst with a sufficient potential to achieve overall H_2O splitting is known as a one-step mechanism (Maeda *et al.* 2005). As previously discussed, the photocatalyst employed should have a suitable thermodynamic potential for H_2O splitting, a sufficiently narrow band gap to harvest visible photons, and stability against photocorrosion. These requirements are rather stringent and thereby limit the number of photocatalysts capable of photosplitting H_2O using the one step mechanism (Maeda *et al.* 2005; Lee *et al.* 2007). Discussed here is the two-step Z-scheme mechanism for H_2O splitting, Figure 13. This dual photocatalyst system for the photosplitting of H_2O was first suggested by Bard in 1979 (Bard 1979). A wider range of visible light is available because a change in Gibbs free energy required to drive each photocatalyst can be reduced when compared to the one step system. It is also possible to separate evolved H_2 and O_2 which is a significant advantage with a view towards large scale H_2 production. The problem of spontaneous backward reaction of redox products remains as in ordinary single-photocatalyst systems. Hence a useful system without any disadvantages has yet to be developed (Sayama *et al.* 2001; Kato *et al.* 2004; Abe *et al.* 2005; Higashi *et al.* 2008; Sasaki *et al.* 2009; Abe *et al.* 2009; Maeda *et al.* 2010; Tabata *et al.* 2010).

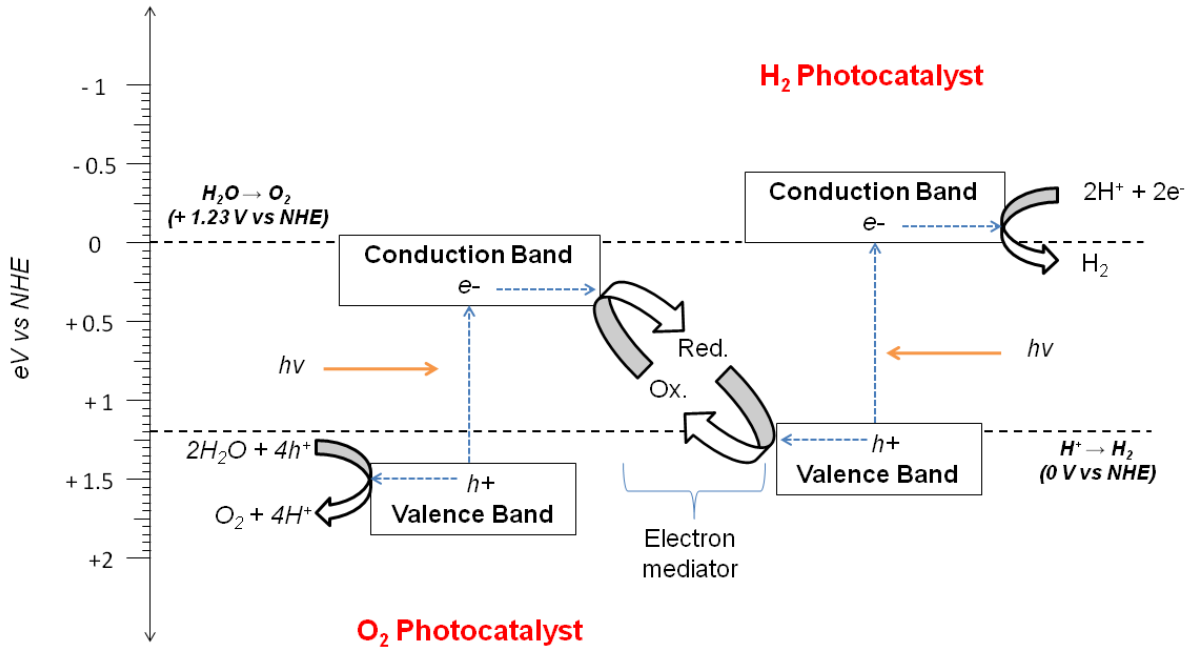

Figure 13; Schematic of Z-scheme photocatalytic process

Two step Z scheme H_2O splitting systems have a number of advantages over conventional one-step systems and currently appear to be the most promising way of achieving efficient H_2O splitting under visible light. Sayama *et al.* reported evidence of the photosplitting of H_2O into H_2 and O_2 using a Z-

scheme photocatalytic system and visible light irradiation (Sayama *et al.* 2001; Sayama *et al.* 2002; Abe *et al.* 2001). $SrTiO_3$ doped with Cr and Ta ($SrTiO_3$:Cr/Ta) for H_2 evolution, WO_3 for O_2 evolution and an iodate/iodide redox couple used as an electron mediator was capable of photosplitting H_2O under visible light. A version of the Z scheme had been previously reported under UV irradiation using Pt loaded anatase TiO_2 and bare rutile TiO_2 photocatalysts in the presence of iodate/iodide redox shuttle (Abe *et al.* 2005). This system was only capable of operation at wavelengths < 400 nm. The large band gap of TiO_2 however meant that there was potential to extend this to the visible light region by appropriate doping of TiO_2 or inclusion of suitable visible light active catalysts.

The simultaneous evolution of H_2 and O_2 in a Z scheme H_2O splitting system is difficult to achieve because the backward reactions of the redox mediator proceed readily over both photocatalysts and suppress the forward reactions (evolution of H_2 and O_2). Hence a redox shuttle is employed.

The most common redox shuttle employed within Z scheme photocatalysis is the IO_3^-/I^- redox shuttle or the Fe^{3+}/Fe^{2+}. They facilitate this via the following reactions:

IO_3^-/I^-:

$$hv \rightarrow e_{CB^-} + h_{VB^+} \qquad \text{Equation (4)}$$

$$IO_3^- + 3H_2O + 6e_{CB^-} \rightarrow I^- + 6OH^- \qquad \text{Equation (5)}$$

$$2H_2O + 4h_{VB^+} \rightarrow O_2 + 4H^+ \qquad \text{Equation (6)}$$

Fe^{3+}/Fe^{2+}

$$Fe^{3+} + e_{CB^-} \rightarrow Fe^{2+} \qquad \text{Equation (7)}$$

$$2H^+ + 2e_{CB^-} \rightarrow H_2 \qquad \text{Equation (8)}$$

$$Fe^{2+} + h_{VB^+} \rightarrow Fe^{3+} \qquad \text{Equation (9)}$$

Early reports of the use of the iodate/iodide redox couple demonstrated the advantage for the photosplitting of H_2O. Sayama *et al.* have reported O_2 evolution over four TiO_2 photocatalysts (A:anatase; R:rutile) in an aqueous solution containing 1 mM $NaIO_3$ under UV irradiation (> 300nm, 400 W high pressure Hg lamp) (Darwent and Mills 1982). Evolution of O_2 over rutile TiO_2 preceded at a steady rate until the amount of O_2 produced reached 1500 μmol in the absence of NaI, this was

also observed in the presence of a significant amount of I^- anions. The amount of O_2 recorded agreed with the stoichiometric amounts expected based on the quantity of IO_3^- added to the solution before irradiation. The results when the photocatalyst used was Pt/WO_3 proceeded in a similar manner. For both catalysts when the amount of I^- was increased the O_2 evolution rate was reduced.

Also reported was the fact that the addition of excess I^- to the solution completely suppressed O_2 evolution over both anatase TiO_2 and $Pt/BiVO_4$ photocatalysts. The loading of a co-catalyst such as Pt or RuO_2 is necessary for the efficient evolution of O_2 over the WO_3 photocatalyst using IO_3^- anion as an electron acceptor. It has been reported that WO_3 alone is capable of O_2 generation from H_2O in the presence of other electron acceptors such as Ag^+ or Fe^{3+} (Erbs *et al.* 1984; Sayama *et al.* 1997; Kato *et al.* 2004). The presence of the Pt co-catalyst mainly serves to provide reduction sites that enable the 6 electron reduction of IO_3^- to I^-.

The use of a photocatalyst combination that favourably adsorbs either IO_3^- or I^- leads to the photosplitting of H_2O via a two step mechanism. The first step involves the reduction of H_2O to H_2 and oxidation of I^- to IO_3^- over a Pt/anatase TiO_2 photocatalyst while the second step involves reduction of IO_3^- to I^- and oxidation of H_2O to O_2 over a rutile TiO_2 photocatalyst.

The rapid reduction of IO^{3-} to I^- over rutile TiO_2 results in a very low IO_3^- concentration during the reaction. This effectively suppresses the undesirable backward reaction (IO_3^- reduction to I^-) over the Pt/anatase TiO_2 photocatalyst giving a higher H_2 evolution rate. The key for achieving H_2O splitting is to use different oxidation reactions; in other words, preferential oxidation of I^- to IO_3^- over the H_2 photocatalyst (e.g., Pt/anatase TiO_2) and preferential oxidation of water to O_2 over the O_2 photocatalyst (e.g., rutile TiO_2) must occur simultaneously in a single solution.

Another major redox couple used to facilitate the two step process of the Z-scheme during photosplitting of H_2O is Fe^{3+}/Fe^{2+}. Kato *et al.* reported H_2O splitting under visible light using a Z-scheme photocatalytic system that consisted of Rh-doped $SrTiO_3$ ($SrTiO_3$:Rh) for H_2 evolution, $BiVO_4$ for O_2 evolution, and a Fe^{3+}/Fe^{2+} redox couple as an electron mediator (Kato *et al.* 2007; Sasaki *et al.* 2008; Ohno *et al.* 1997). Previous studies had demonstrated the functionality of using Fe^{3+} ions as efficient electron acceptors over a RuO_2/WO_3 or rutile TiO_2 photocatalyst for O_2 evolution (Kato *et al.* 2004; Konta *et al.* 2004). However, the use of Fe^{2+} ions as electron donors for the efficient photocatalytic production of H_2 had not previously been achieved.

Doping with Rh cations (Ishii *et al.* 2004) and co-doping with Cr^{3+}/Ta^{5+} (Kato and Kudo 2002), Cr^{3+}/Sb^{5+} (Kato and Kudo, 2002), and Ni^{2+}/Ta^{5+} has been reported to sensitise $SrTiO_3$ to visible light. Kudo *et al.* demonstrated that doped $SrTiO_3$ powders with Pt-co-catalyst exhibit photocatalytic activities for H_2 evolution under visible light. This proceeds in the presence of methanol as a sacrificial electron donor. Pt-loaded $SrTiO_3$:Rh photocatalyst demonstrated activity for H_2 evolution

from H_2O in the presence of Fe^{2+} as a reversible electron donor. The reaction was initiated in $FeCl_3$ aq. (2 $mmolL^{-1}$), predominantly produced O_2 during the initial stage of the first run. The rate of O_2 production subsequently decreased gradually. In a second run after evacuation of the gas phase, H_2 and O_2 were produced in the stoichiometric ratio (2:1) during the initial period. The reaction in $FeCl_2$ aq. (2 $mmolL^{-1}$) also exhibited stoichiometric evolution of H_2 and O_2 during the second run, while H_2 was predominantly evolved in the initial stage of the first run. In both cases, Fe^{3+} and Fe^{2+} ions in the steady state were found to have concentrations of ca. 1.5 and 0.5 $mmolL^{-1}$, respectively. H_2 and O_2 can be evolved in the ($Pt/SrTiO_3$:Rh)–($BiVO_4$) system even when the reductant (Fe^{2+}) and the oxidant (Fe^{3+}) coexist. This differs significantly when compared to the IO^{3-}/I^- redox couple, where H_2 production is suppressed by the coexistence of a small amount of oxidant (IO^{3-}) due to preferential re-reduction of IO^{3-} anions over water by the photoexcited electrons (Sayama *et al.* 2001; Sayama *et al.* 2002; Darwent and Mills 1982).

This demonstrates that the H_2 photocatalyst ($Pt/SrTiO_3$:Rh) and the O_2 photocatalyst (BiVO4) have sufficiently high selectivities for the forward reactions. H_2 evolution on the Pt/SrTiO3:Rh photocatalyst was enhanced rather than suppressed by the presence of Fe^{3+} (Sasaki *et al.* 2008). The results of investigations of photocatalytic H_2 evolution and dark reactions in various aqueous solutions containing Fe^{3+} ions strongly suggest that the adsorption of $[Fe(SO_4)(H_2O)_5]^+$ and/or $[Fe(OH)(H_2O)_5]^{2+}$ on the Pt surface efficiently suppresses both the undesirable backward reactions on the Pt surface, water formation from H_2 and O_2, and the reduction of Fe^{3+} with H_2. The increased H_2 production that accompanies an increase in the Fe^{3+} ion concentration is somewhat unusual in view of the electron acceptability of Fe^{3+}. The beneficial effect of Fe^{3+} suppressing the backward reactions should exceed the detrimental effect of Fe^{3+} trapping photoexcited electrons. In contrast to H_2 evolution, O_2 evolution over the $BiVO_4$ photocatalyst was remarkably inhibited by the presence of Fe^{2+} ions, indicating that oxidation of Fe^{2+} to Fe^{3+} on the $BiVO_4$ photocatalyst (Sasaki *et al.* 2008). $BiVO_4$ has a sufficiently high selectivity for the forward reaction, which enables O_2 production even when there is a high (5 mmol L^{-1}) Fe^{2+} ion concentration. The splitting of H_2O under visible light has also been achieved using WO_3 or Bi_2MoO_6 as an O_2 evolution photocatalyst in combination with a $Pt/SrTiO_3$:Rh photocatalyst in the presence of Fe^{3+}/Fe^{2+} electron mediator (Kato *et al.* 2007). Challenges remain in the promotion of electron transfer between two semiconductors and in the suppression of backward reactions involving shuttle redox mediators.

3 Water splitting mechanism

3.0 Multimolecular systems

3.0.1 Ideal functions

H_2 and/or O_2 production from H_2O by visible light requires one or several intermediates having ideally the following functions:

1. Visible light absorption,
2. Conversion of the excitation energy to redox energy (charges),
3. Concerted transfer of several electrons to water leading to the formation of H_2 as energy-storage compound and/or to the formation of O_2.

Indeed, one of the main difficulties in achieving the splitting of H_2O by means of light-induced redox processes is that H_2 requires two electrons Equation (10) while O_2 requires four electrons, Equation (11).

$$2H_2O + 2e^- \rightarrow H_2 + 2OH^-, E^\circ(pH = 7) = -0.41\ vs\ NHE \qquad \text{Equation (10)}$$

$$2H_2O \rightarrow O_2 + 4H^+ + 4e^-, E^\circ(pH = 7) = +0.82\ vs\ NHE \qquad \text{Equation (11)}$$

This number of charges corresponds to the most favourable thermodynamic conditions for Equation (1). The reaction is a multi-electron transfer process which requires 1.23 eV per electron transferred. Hence, photons with $\lambda < 1008$ nm corresponding to a minimum energy of 1.23 eV can induce the cleavage of H_2O.

As has been previously discussed, upon illumination with light of energy greater than the E_g, a semiconductor will form electrons and holes. The E_g is the energy difference between the VB and the CB. The electron and holes formed are highly charged and initiate reduction and oxidation reactions. H_2O molecules are reduced by the electrons to form H_2 and are oxidised by the holes to form O_2 for overall H_2O splitting.

3.0.2 General schemes for H_2 and O_2 production

Early research reported photochemical systems involving several compounds. A multi-molecular system was designed with each compound fulfilling a particular role towards the photosplitting of

H_2O. The first compound required was a photosensitiser (PS) capable of visible light absorption in order to generate the excited species PS* with useful redox properties, Equation (12):

$$PS \xrightarrow{h\nu_{vis}} PS^* \qquad \text{Equation (12)}$$

A second compound R is necessary which can be reduced or oxidized by quenching of the excited species PS* in electron transfer reactions. This leads to the formation of charge pairs, PS^+, R^- in the case of the oxidative quenching of PS, Equation (13):

$$PS^* + R \rightarrow PS^+ + R^- \qquad \text{Equation (13)}$$

Finally it requires a third compound capable of collecting several electrons to facilitate the exchange of two or four electrons with water. This multi-electron collection and transfer can be realised by a specific redox catalyst.

$$2R^- + 2H^+ \xrightarrow{Cat} 2R + H_2 \qquad \text{Equation (14)}$$

In such a system, the second compound R acts as an electron relay between the photosensitizer PS and the catalyst (Cat) mediating the electron collection. The redox potential of its reduced species R - must be less than - 0.41 V (*vs* NHE, pH = 7) to take part in Equation (10).

The main problem associated with this process is the fast recombination of charge pairs, Equation (15).

$$PS^+ + R^- \rightarrow PS + R \qquad \text{Equation (15)}$$

The main challenge for these multi-molecular systems is how to prevent the back electron transfer reaction in order to increase the charge separation lifetime.

In the case of multi-molecular systems, the introduction of a fourth compound in the form of an electron donor should help to prevent this back reaction. The electron donor should scavenge the oxidized photosensitizer PS^+ in a competitive electron transfer reaction to give the initial PS and a donor oxidation product D^+, Equation (16).

$$PS^+ + D \rightarrow PS + D^+ \qquad \text{Equation (16)}$$

$$D^+ \rightarrow Products \qquad \text{Equation (17)}$$

The latter is a sacrificial system and rapidly decomposes irreversibly, Equation (8). D is the only compound, apart from H_2O (H^+), which is consumed. The other compounds PS, R and Cat follow catalytic cycles.

Two schemes for cyclic production of H_2 from H_2O were proposed (Higashi *et al.* 2008). The first called the "oxidative quenching mechanism" involved oxidation of the excited photosensitizer PS* to PS^+ by the electron relay R, Figure 14 a. It corresponds to reaction, Equation (12) to Equation (17).

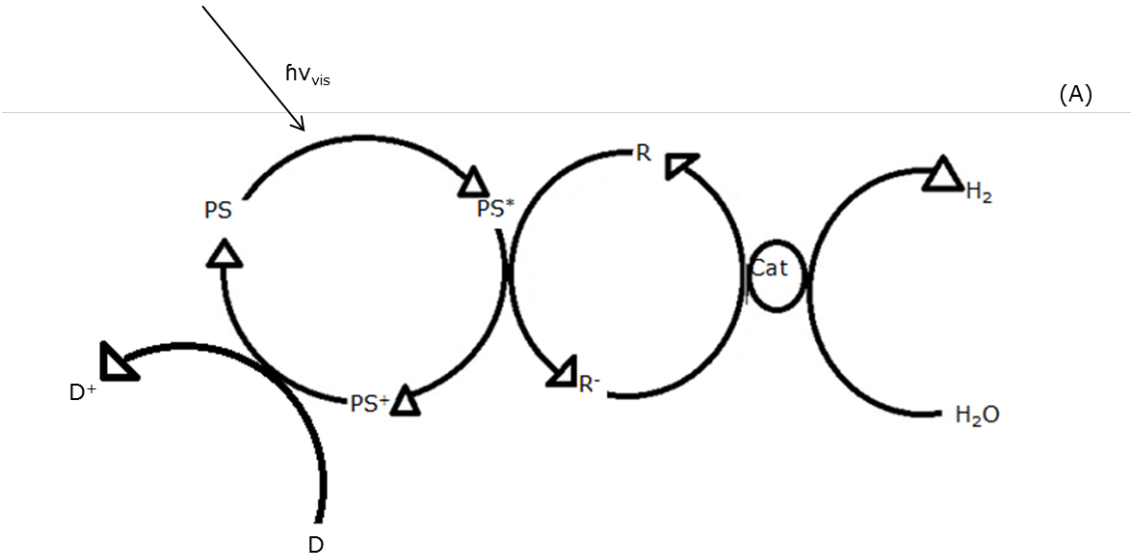

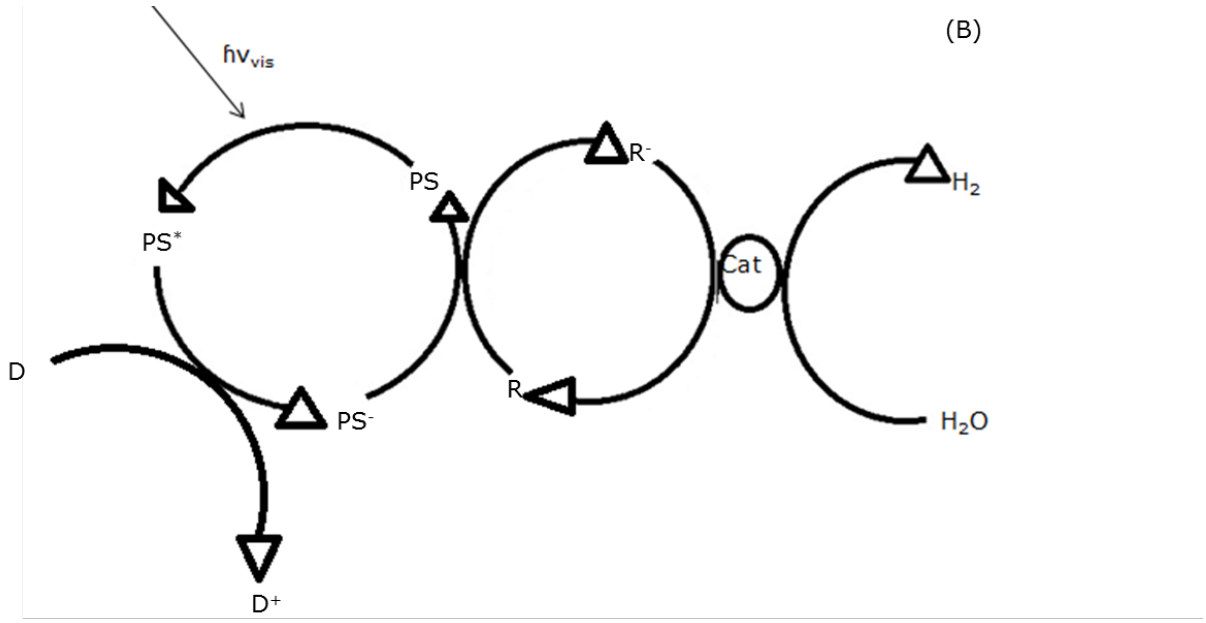

Figure 14; Schematic representation of the redox catalytic cycles in the photoreduction of H_2O to H_2 by visible-light irradiation of a four-component model system PS/R/D/Cat: (a) oxidative quenching mechanism (b) reductive quenching mechanism (reproduced from Higashi *et al*. (2008), with kind permission of Elsevier)

The reduction of the excited state photosensitizer PS*' by D is called reductive quenching (Figure 14 b).

$$PS^* + D \rightarrow PS^- + D^+ \qquad \text{Equation (18)}$$

This primary reaction, Equation (18), yields the reduced photosensitizer PS^- and the oxidized donor D^+ which decompose irreversibly, Equation (17). In this way, PS^- can accumulate and react with an electron relay R to regenerate PS and to yield R^-, Equation (19).

$$PS^- + R \rightarrow PS + R^- \qquad \text{Equation (19)}$$

The inclusion of a suitable catalyst allows the formation of R^- which can lead to the production of H_2 as is shown in Equation (14).

PS^- is a more powerful reducing species than R^-. Therefore the reduction of H_2O to H_2 can be achieved directly by PS^- itself in the presence of a suitable catalyst. As a consequence, this scheme involves only three components (PS, D, Cat) and the mechanism becomes simplified (Figure 15).

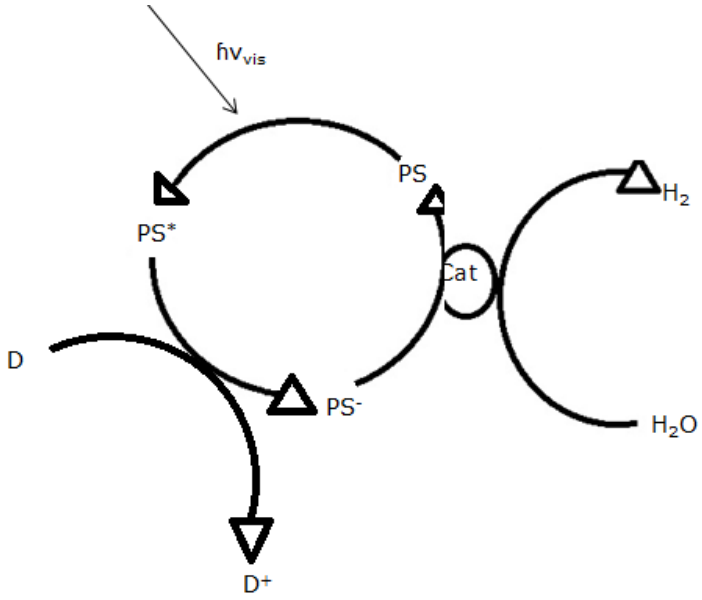

Figure 15; Redox catalytic cycles in the photoreduction of H_2O to H_2, via reductive quenching mechanism for a three component model system PS/D/Cat (reproduced from Higashi *et al*. (2008), with kind permission of Elsevier)

Similar three-component systems for O_2 production from water have been proposed (Figure 16). These systems require the formation, following visible-light excitation of the photosensitizer PS, of a strong oxidizing species PS^+, having a redox potential E° (PS^+/IPS*)* greater than 0.82 V (*vs* NHE, pH = 7). This can be achieved by using an electron-acceptor A as quencher which, once reduced to A^-, Equation (20), decomposes irreversibly, Equation (21).

$$PS^+ + A \rightarrow PS^+ + A^- \qquad \text{Equation (20)}$$

$$A^- \rightarrow Decomposition\ products \qquad \text{Equation (21)}$$

The oxidized PS^+ can accumulate and lead to O_2 evolution in the presence of a suitable catalyst capable of facilitating the exchange of 4 electrons with H_2O, Equation (22).

$$4PS^{+} + 2H_2O \xrightarrow{Cat} 4PS + 4H^{+} + O_2$$ Equation (22)

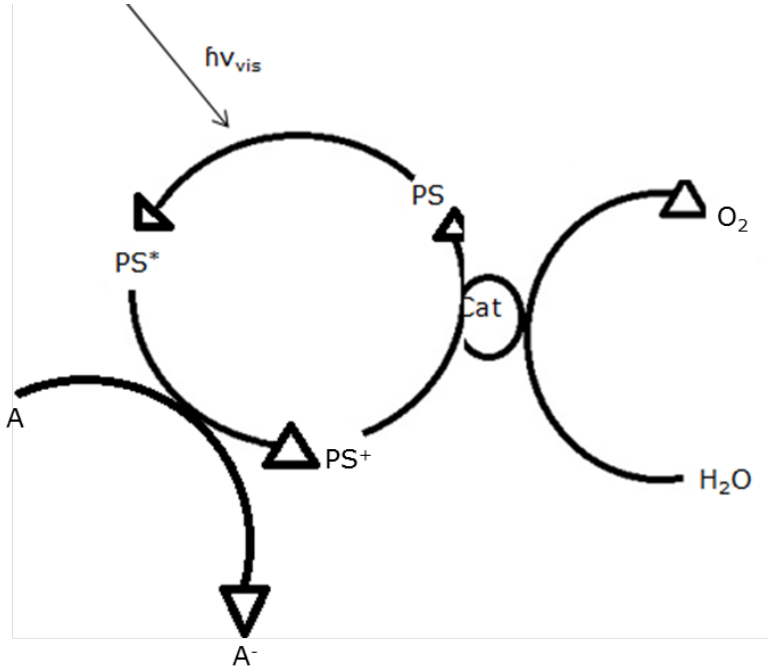

Figure 16; Redox catalytic cycles in the photooxidation of H_2O to O_2 by visible-light irradiation of a three-component model system PS/A/Cat (reproduced from Higashi *et al*. (2008), with kind permission of Elsevier)

3.1 Recent developments

In recent years research into the development of materials capable of photosplitting of water have focused on two approaches:

1. One step mechanism
2. Two step mechanism

The one step mechanism is shown in Figure 3, while the two step Z-scheme mechanism is represented in Figure 13.

3.1.1 One step mechanism

The one-step mechanism of H_2O photosplitting into H_2 and O_2 uses a single visible light active photocatalyst. However there are very few stable semiconductor materials available to achieve photosplitting of H_2O with a one-step mechanism. Band engineering of semi-conductors is required to artificially develop new semiconductor materials that would satisfy the following criterion:

1. Have a narrow band gap
2. Stable under photo-irradiation
3. Suitable conduction and valence band levels for H_2 and O_2 production.

It is impossible in principle to achieve separate production of H_2 and O_2 in a conventional one step water splitting system as H_2 and O_2 are evolved simultaneously on small semiconductor particles.

3.1.2 Two step mechanism

A process inspired by natural photosynthesis in green plants is the two-step mechanism of photosplitting of water, known as the Z scheme. This mechanism uses two different photocatalysts one tailored for H_2 production and the other for O_2 production and water is split into stoichiometric amounts of H_2 and O_2 in combination with a redox couple in the solution.

Within this system the photocatalyst for H_2 production the photoexcited electrons reduce water to H_2 and the holes in the valence band oxidise the reductant (Red) to an oxidant (Ox). The oxidant is reduced back to the reductant by photoexcited electrons over and O_2 evolving photocatalyst where the holes oxidise H_2O to O_2. This system allows a semi-conductor to be used that has either a water reduction or oxidation potential on one side of the system. As a result of this a variety of semi-conductors can be used on the Z-scheme even if they do not satisfy all the stringent requirements for a one-step system.

Another advantage of Z scheme systems is the ability to separate production of H_2 and O_2 by employing a separator, such as porous glass filter, that permits only redox mediators to be transferred. A disadvantage of Z scheme systems as this is a two step photoexcitation system the number of photons needed to achieve water splitting is 2 fold larger than with the one step system.

4 Photoreactors for water splitting

The splitting of H_2O on illuminated semiconductors has long been studied as a clean and renewable means of converting solar energy into chemical energy in the form of H_2. The production of H_2 from H_2O through chemistry has been known for hundreds of years, the United States military has been using a ferrosilicon reaction since the first world war (Weaver *et al.*). NaOH, ferrosilicon and H_2O are added to a sealed vessel and as the hydroxide dissolves and heats to 200 ^oF, H_2 and steam are produced. Many other methods are also used, steam reforming, CO_2 sequestration, partial oxidation, plasma reforming, coal, electrolysis, photobiological, sulphur-iodine, fermentative production, enzymatic production, renewable hydrogen and lastly photocatalysis (Guo and Chen 2011; Musa *et al.*

2014; Kumar *et al.* 2013; Sugai *et al.* 2012; Huang *et al.* 2013; Ge *et al.* 2013; Bundaleska *et al.* 2013; Kim *et al.* 2014; Liberatore *et al.* 2012). Photocatalytic H_2O splitting through two-step photoexcitation using two different semiconductor materials and a reversible donor-acceptor pair is one of the possible forms of "manmade photosynthesis" and is known as the Z-scheme system, which was described previously and can be seen in Figure 13. The development of new semiconductor materials aids in the efficiency of Z-scheme H_2O splitting by reducing the number of back reactions. This section shall focus on reactors developed for H_2O splitting primarily with a view towards the production of H_2 via a photoelectrochemical system.

4.0 Photochemical reactors

Photoreactors utilising a catalyst suspension has advantages over a photoelectrochemical cell, a higher surface area which results in more active sites for photocatalytic reactions to take place, also it is a far more simple process as no film deposition or coating is required.

Photocatalytic H_2O splitting can be divided into two types of reaction, photochemical and photoelectrochemical. The photochemical is more commonly referred to as taking place in a photoreactor or photocatalytic reactor, which consists of a powder catalyst in a suspension in an aqueous media. Whereas a photoelectrochemical cell (PEC) consists of an immobilised photocatalyst on an anode.

Photoreactors for the splitting of H_2O take many forms, utilise numerous shapes and sizes of vessels and utilise many materials. These can range from the simplest of set up, single chamber reactor, Figure 17, to the more complex multi-chambered multi-layer cell type. Whatever design, the housing of the reactor takes, the fundamental operational principles remain the same, and it is those which shall be addressed here.

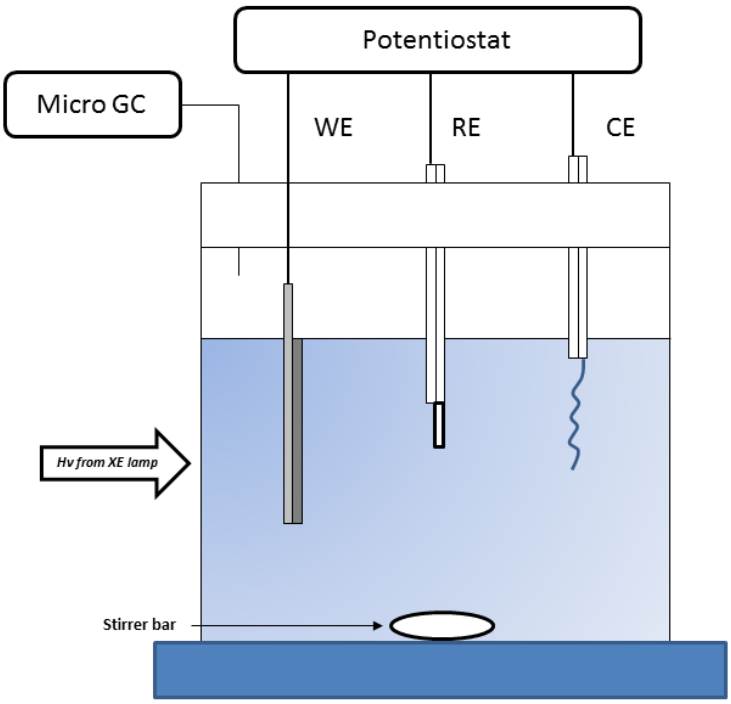

Figure 17; Single chamber triple electrode PEC reactor (reproduced from Xing *et al.* (2013), with kind permission of Elsevier)

The most basic form of reactor is the beaker or cube shaped vessel, the latter tends to be more acceptable as curved surfaces are not suitable for electrode style set ups. The biggest drawback of a single chambered (or non-membrane) reactor is the dangerous mixture of O_2 and H_2. This is quite possibly the single biggest danger in H_2O splitting, the mixture of O_2/H_2 forming an explosive ratio. In the case of batch or stirred tank photoreactors this proves to be the greatest danger but also the more complex problem, as separating H_2 and O_2 requires expensive membrane technology or cryo processing (Zhang *et al.* 2013; Yu *et al.* 2011).

It can be seen in Figure 18 that it is possible to use a batch style stirred photoreactor to produce H_2 and O_2 in the same system, but the two gases are generated in isolation thanks to a proton membrane such as Nafion.

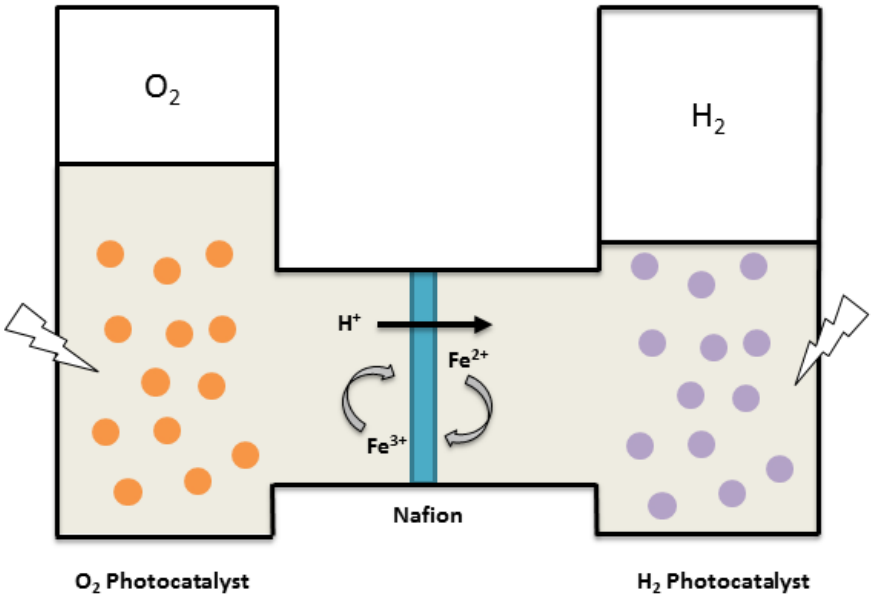

Figure 18; Bi-gas sulfonated tetrafluoroethylene membrane cell (reproduced from Liao *et al*. (2012), with kind permission of International Association of Hydrogen Energy)

The same principles of format can be applied to multi-chambered PEC reactors, Figure 19. The use of coated electrodes for the generation of H_2 and O_2 can be seen in a twin chamber and triple chamber arrangement.

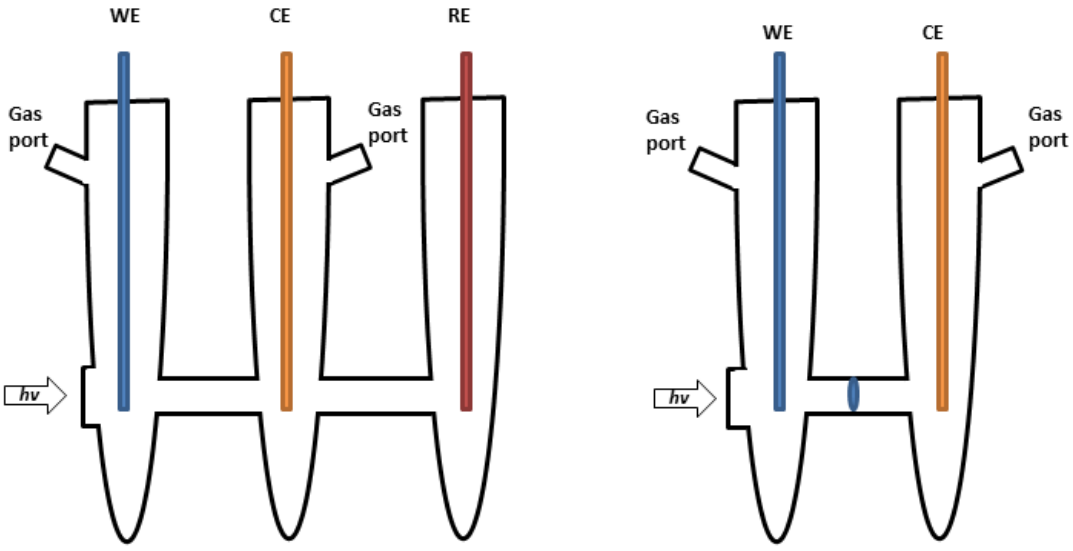

Figure 19; H-type reaction vessels, triple and twin chamber (reproduced from Minggu *et al*. (2010), with kind permission of International Association of Hydrogen Energy)

In the triple chamber reaction vessel the H_2 and O_2 are evolved on the WE and CE electrodes in ported chambers under illumination via a side window, this arrangement of porting prevents explosive mixing of the two gases. Similarly in the twin chamber reactor, the evolution of gas occurs on the WE and CE electrodes but this time the reactor contains a Nafion membrane which allows the H^+ to transfer to the CE side of the reactor.

There are many other formats of photochemical reactors which contain the same constituent components but vary the orientation and design (Matsumoto *et al.* 2012; Zhang *et al.* 2010; Lo *et al.* 2010; Yu *et al.* 2011; Jing *et al.* 2010; Huang *et al.* 2012; Yan *et al.* 2011; Babu *et al.* 2012; Ding *et al.* 2013).

4.1 Photoelectrochemical cell reactors

In a photoelectrochemical cell reactor the catalyst is prepared in a thin film on a substrate to form a photo-anode, with the application of an external circuit to direct the electrons from the photocatalyst to the cathode where H_2 is evolved, Figure 20.

The mechanism involves fundamentally 4 steps

1. Generation of electron hole pairs on the photo-anode
2. Oxidation of water by the holes to give O_2 and H^+
3. Transfer of photogenerated electrons circulate to cathode
4. Reduction of H^+ on cathode to give H_2

The first demonstration of this type of PEC was by Fujishima and Honda in 1972. The photoelectrochemical reactor is a bi-gas system where O_2 is generated, on the anode from the splitting of H_2O.

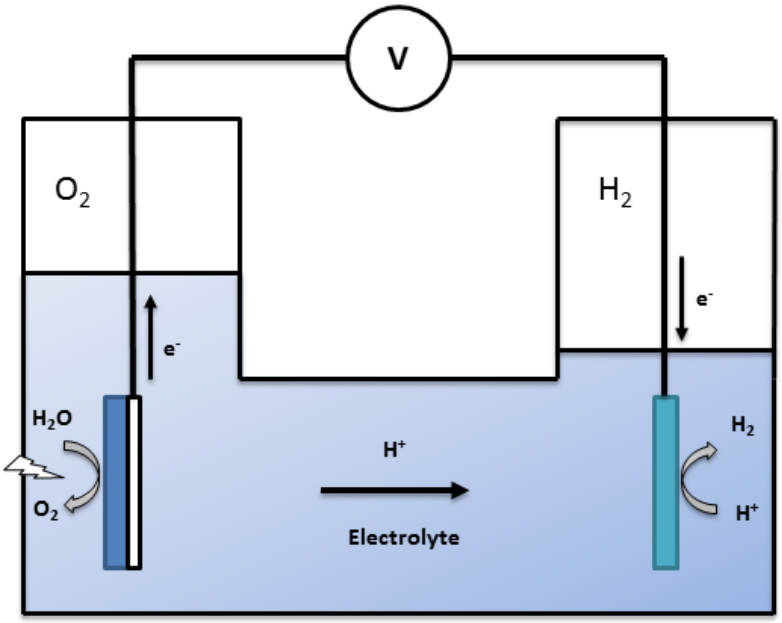

Figure 20; Schematic of photoelectrochemical cell (reproduced from Liao *et al*. (2012), with kind permission of International Association of Hydrogen Energy)

The major advantage of a PEC is the ability to create bias within the cell by altering the anode material configuration. The internal bias can be further complemented by applying an external bias between the electrodes. Water, under certain conditions, can be reversibly electrolysed at a potential of 1.23 V.

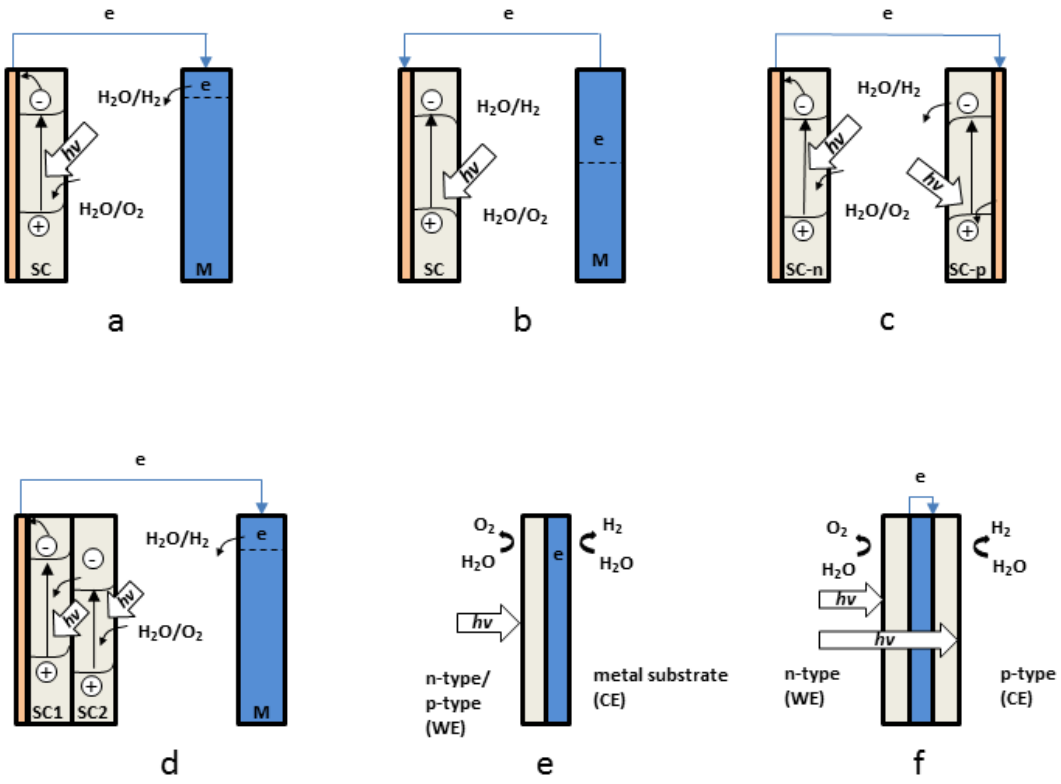

Figure 21; Types of photoelectrochemical cells, (a) n-type, (b) p-type, (c) n-&p-type, (d) hybrid, (e) monolithic-bypolar and (f) monolithic-electrical connection (reproduced from Minggu *et al*. (2010), with kind permission of International Association of Hydrogen Energy)

Semiconductors are the main photoactive material in a PEC and can be classified as either metal oxide or photovoltaic material. There are several types of PEC which exist; n-type, p-type, n-&p-type, hybrid, monolithic-bypolar and monolithic-electrical connection, Figure 21. For example an n-type semiconductor can be TiO_2 (a), p-type can be InP (b) and a n-&p-type can be n-GaAs/p-InP (c). A hybrid cell could consist of several n-type semiconductors with differing band gaps to cover more of the solar electromagnetic spectrum (d). It is possible to also have a hybrid cell which combines both the anode and cathode in a monolithic structure (e) with a metal substrate coated on either side or to separate the anode and cathode with their own isolated substrate and connect the two with an electrical connection (f) (He *et al.* 2014; Li *et al.* 2013; Zhu *et al.* 2013; Danko *et al.* 2013; Wang *et al.* 2014; Zhang *et al.* 2014).

4.1.1 Cell biasing

The optimum PEC is the generation of H_2 without the application of an external current. This zero biasing only occurs when the band gap and band edges of the photocatalyst is correct to split H_2O. Currently there is no single semiconductor which can produce H_2 in a sufficient quantity under a zero bias operation, the application of an external current is necessary to create viability (Li *et al.* 2011; Hsu *et al.* 2011).

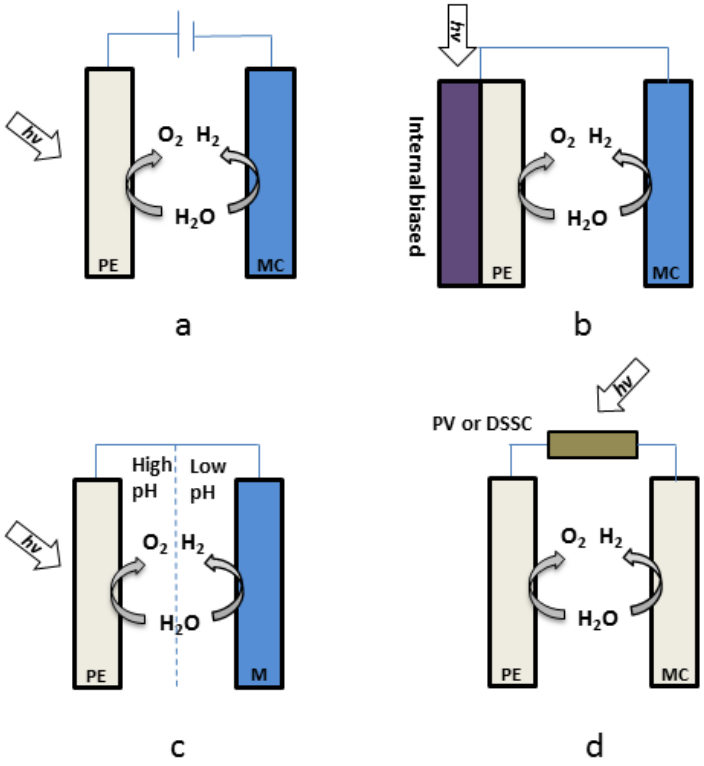

Figure 22; Biasing methods for photoelectrochemical water splitting (reproduced from Minggu *et al.* (2010), with kind permission of International Association of Hydrogen Energy)

There are several types of external bias which can be applied to a PEC including an electrical bias, chemical bias, photovoltaic bias or internal bias, Figure 22. In the case of electrical bias (a), the PEC is connected to an external power supply. In practice this is a reliable and effective method of biasing a PEC, but ultimately defeats the green energy credentials of photocatalytic sytems; unless driven via renewable sources. For an internally biased PEC (b), it is the multilayer structure of the anode which creates the required bias. This can take the form of PV~a-SiGe, PEC~WO_3, PV_1~GaInP, PV_2~GaAs or PEC/PEC PEC_1~DSSC PEC_2~WO_3 whereby the structures achieve the correct band gap required. In the case of chemical bias (c) the pH of the electrolyte which the anode and cathode are submerged,

separated by an ion exchange membrane, acid one side and alkali on the other. This form of biasing proves un-cost effective as a constant replenishing of the starting electrolytes is required as each move towards equilibrium as H^+ and OH^- are consumed. For photovoltaic bias (d), a solar photovoltaic cell is directly connected to the PEC, this could be a dye sensitised cell for example (Andrade *et al.* 2010; Shin *et al.* 2013; Abe *et al.* 2010; Lianos *et al.* 2011).

4.1.2 Photovoltaic photoelectrochemical cell

As mentioned in the previous section, an increasingly common format for a PEC is the addition of a photovoltaic cell as shown in Figure 23. For realistic low impact H_2 production from H_2O spitting, the use of a photovoltaic cell allows a more energy efficient process to occur (Fujii *et al.* 2013; Zhang *et al.* 2012; Avachat *et al.* 2006; Mishra *et al.* 2007). Recent research has shown an increase in photovoltaic efficiency in the region of 12% (Gibson and Kelly, 2008).

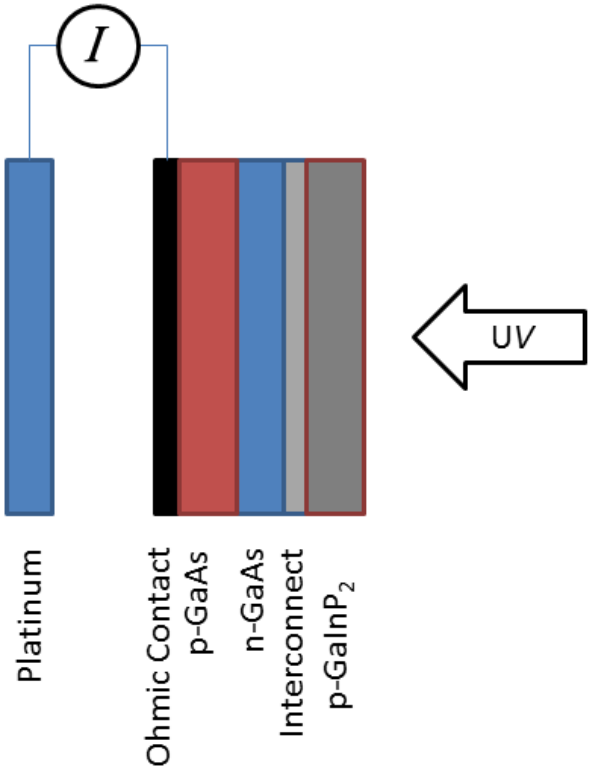

Figure 23; Monolithic photoelectrochemical/photovoltaic device (reproduced from Liao *et al.* (2012), with kind permission of International Association of Hydrogen Energy)

4.2 Illumination

There are several laboratory based illumination sources currently employed in water splitting, ultra-violet, visible and solar simulator lamps are used with bench scale systems. In the case of larger scale up systems a move towards purely natural solar illumination is necessary as there is no economic viability in creating purely lamp driven H_2. As the solar electromagnetic spectrum contains ~4 % UV and almost 50 % visible light the move towards visible absorbing catalyst is needed to make photocatalytic water splitting a viable technology. Current catalyst trends are directing formulation towards visible only activation, but efficiencies are still low for commercially viable catalysts.

5 References

ABE, R., SHINMEI, K., HARA, K. and OHTANI, B., 2009. Robust Dye-Sensitized Overall Water Splitting System with Two-Step Photoexcitation of Coumarin Dyes and Metal Oxide Semiconductors. *Chemistry Communications,* , pp. 3577-3579.

ABE, R., TAKATA, T., SUGIHARA, H. and DOMEN, K., 2005. Photocatalytic OverallWater Splitting under Visible Light by TaON andWO3 with an IO3-/I- Shuttle Redox Mediator. *Chemistry Communications,* , pp. 3829-3831.

ABE, R., 2010. Recent progress on photocatalytic and photoelectrochemical water splitting under visible light irradiation. *Journal of Photochemistry and Photobiology C: Photochemistry Reviews,* 11(4), pp. 179-209.

ABE, R., HIGASHI, M., SAYAMA, K., ABE, Y. and SUGIHARA, H., 2006. Photocatalytic Activity of R3MO7 and R2Ti2O7 (R) Y, Gd, La; M) Nb, Ta) for Water Splitting into H2 and O2. *Journal of Physical Chemistry B,* 110(5), pp. 2219-2226.

ABE, R., SAYAMA, K., DOMEN, K. and ARAKAWA, H., 2001. A new type of water splitting system composed of two different TiO_2 photocatalysts (anatase, rutile) and a IO_3^-/I^- shuttle redox mediator. *Chemical Physics Letters,* 344(3), pp. 339-344.

ABE, R., SAYAMA, K. and SUGIHARA, H., 2005. Development of new photocatalytic water splitting into H2 and O2 using two different semiconductor photocatalysts and a shuttle redox mediator IO_3^-/I^-. *Journal of Physical Chemistry B,* 109, pp. 16052-16061.

ALAM KHAN, M., SHAHEER AKHTAR, M., WOO, S.I. and YANG, O., 2008. Enhanced photoresponse under visible light in Pt ionized TiO2 nanotube for the photocatalytic splitting of water. *Catalysis Communications,* 10(1), pp. 1-5.

ALTOMARE, M., POZZI, M., ALLIETA, M., BETTINI, L.G. and SELLI, E., 2013. H2 and O2 photocatalytic production on TiO2 nanotube arrays: Effect of the anodization time on structural features and photoactivity. *Applied Catalysis B: Environmental,* 136–137(0), pp. 81-88.

AMOUYAL, E., 1995. Photochemical production of hydrogen and oxygen from water: A review and state of the art. *Solar Energy Materials and Solar Cells,* 38(1–4), pp. 249-276.

ANDRADE, L., CRUZ, R., RIBEIRO, H.A. and MENDES, A., 2010. Impedance characterization of dye-sensitized solar cells in a tandem arrangement for hydrogen production by water splitting. *International Journal of Hydrogen Energy,* 35(17), pp. 8876-8883.

ARAI, N., SAITO, N., NISHIYAMA, H., DOMEN, K., KOBAYASHI, H., SATO, K. and INOUE, Y., 2007. Effects of divalent metal ion (Mg2+, Zn2+ and Be2+) doping on photocatalytic activity of ruthenium oxide-loaded gallium nitride for water splitting. *Catalysis Today,* 129(3–4), pp. 407-413.

AVACHAT, U.S., JAHAGIRDAR, A.H. and DHERE , N.G., 2006. Multiple bandgap combination of thin film photovoltaic cells and a photoanode for efficient hydrogen and oxygen generation by water splitting. *Solar Energy Materials and Solar Cells,* 90(15), pp. 2464-2470.

BABU, V.J., KUMAR, M.K., NAIR, A.S., KHENG, T.L., ALLAKHVERDIEV, S.I. and RAMAKRISHNA, S., 2012. Visible light photocatalytic water splitting for hydrogen production from N-TiO_2 rice grain shaped electrospun nanostructures. *International Journal of Hydrogen Energy,* 37(10), pp. 8897-8904.

BAE, S.W., JI, S.M., HONG, S.J., JANG, J.W. and LEE, J.S., 2009. Photocatalytic overall water splitting with dual-bed system under visible light irradiation. *International Journal of Hydrogen Energy,* 34(8), pp. 3243-3249.

BANIASADI, E., DINCER, I. and NATERER, G.F., 2013. Hybrid photocatalytic water splitting for an expanded range of the solar spectrum with cadmium sulfide and zinc sulfide catalysts. *Applied Catalysis A: General,* 455(0), pp. 25-31.

BARD, A.J., 1979. Photoelectrochemistry and Heterogenous Photocatalysis at Semiconductors. *Journal of Photochemistry and Photobiology C: Photochemistry Reviews,* 10, pp. 59-75.

BOLTON, J.R., 1996. Solar photoproduction of hydrogen: A review. *Solar Energy,* 57(1), pp. 37-50.

BUNDALESKA, N., TSYGANOV, D., SAAVEDRA, R., TATAROVA, E., DIAS, F.M. and FERREIRA, C.M., 2013. Hydrogen production from methanol reforming in microwave “tornado”-type plasma. *International Journal of Hydrogen Energy,* 38(22), pp. 9145-9157.

CHEN, W., LI, C., GAO, H., YUAN, J., SHANGGUAN, W., SU, J. and SUN, Y., 2012. Photocatalytic water splitting on protonated form of layered perovskites K0.5La0.5Bi2M2O9 (M = Ta; Nb) by ion-exchange. *International Journal of Hydrogen Energy,* 37(17), pp. 12846-12851.

CHIOU, Y., KUMAR, U. and WU, J.C.S., 2009. Photocatalytic splitting of water on NiO/InTaO4 catalysts prepared by an innovative sol–gel method. *Applied Catalysis A: General,* 357(1), pp. 73-78.

DANKO, D.B., SYLENKO, P.M., SHLAPAK, A.M., KHYZHUN, O.Y., SHCHERBAKOVA, L.G., ERSHOVA, O.G. and SOLONIN, Y.M., 2013. Photoelectrochemical cell for water decomposition with a hybrid photoanode and a metal-hydride cathode. *Solar Energy Materials and Solar Cells,* 114, pp. 172-178.

DARWENT, J.,R. and MILLS, A., 1982. Photo-oxidation of water sensitized by WO_3 powder *Journal of chemistry society faraday transcriptions,* 78, pp. 359-367.

DESHPANDE, A., SHAH, P., GHOLAP, R.S. and GUPTA, N.M., 2009. Interfacial and physico-chemical properties of polymer-supported CdS·ZnS nanocomposites and their role in the visible-light mediated photocatalytic splitting of water. *Journal of colloid and interface science,* 333(1), pp. 263-268.

DING, L., ZHOU, H., LOU, S., DING, J., ZHANG, D., ZHU, H. and FAN, T., 2013. Butterfly wing architecture assisted CdS/Au/TiO_2 Z-scheme type photocatalytic water splitting. *International Journal of Hydrogen Energy*, 47(3), pp. 1480-1490.

DING, L., ZHOU, H., LOU, S., DING, J., ZHANG, D., ZHU, H. and FAN, T., 2013. Butterfly wing architecture assisted CdS/Au/TiO2 Z-scheme type photocatalytic water splitting. *International Journal of Hydrogen Energy*, 38(20), pp. 8244-8253.

DOMEN, K., KUDO, A., ONISHI, T., KOSUGI, N. and KURODA, H., 1986. Photocatalytic Decomposition of Water into H2 and 0, over NiO-SrTi0, Powder. 1. Structure of the Catalyst. *Journal of Physical Chemistry*, 90(2), pp. 292-295.

DVORANOVA, D., BREZOVA, V., MAZUR, M. and MALATI, M., 2002. Investigations of metal-doped titanium dioxide photocatalysts. *Applied Catalysis B: Environmental*, 37(2), pp. 91-105.

ERBS, W., DESILVESTRO, J., BORGARELLO, E. and GRATZEL, M., 1984. Visible-Light-Induced O_2 Generation from Aqueous Dispersions of WO_3. *Journal of Physical Chemistry*, 88, pp. 4001.

ESSWEIN, A. and NOCERA, D., 2007. Hydrogen production by molecular photocatalysis. *Chemical Reviews*, 107(10), pp. 4022-4047.

FUJII, K., NAKAMURA, S., SUGIYAMA, M., WATANABE, K., BAGHERI, B. and NAKANO, Y., 2013. Characteristics of hydrogen generation from water splitting by polymer electrolyte electrochemical cell directly connected with concentrated photovoltaic cell. *International Journal of Hydrogen Energy*, 38(34), pp. 14424-14432.

FUJISHIMA, A. and HONDA, K., 1972. Electrochemical photolysis of water at a semiconductor electrode. *Nature*, 238, pp. 37-38.

GE, Z., GUO, S., GUO, L., CAO, C., SU, X. and JIN, H., 2013. Hydrogen production by non-catalytic partial oxidation of coal in supercritical water: Explore the way to complete gasification of lignite and bituminous coal. *International Journal of Hydrogen Energy*, 38(29), pp. 12786-12794.

GIBSON, S.T.L. and KELLY, N.A., 2008. Optimization of solar powered hydrogen production using photovoltaic electrolysis devices. *International Journal of Hydrogen Energy*, 33, pp. 5931-5940.

GUO, J. and CHEN, X., eds, 2011. *Solar Hydrogen Generation: Transition Metal Oxides in Water Photoelectrolysis*. McGraw Hill.

HAGIWARA, H., NAGATOMO, M., IDA, S. and ISHIHARA, T., 2012. Photocatalytic Splitting of Water into Hydrogen and Oxygen on Organic Dye Modified KTa(Zr)O3 Catalyst. *Energy Procedia*, 22(0), pp. 53-60.

HAMEED, A., GONDAL, M.A. and YAMANI, Z.H., 2004. Effect of transition metal doping on photocatalytic activity of WO3 for water splitting under laser illumination: role of 3d-orbitals. *Catalysis Communications*, 5(11), pp. 715-719.

HARA, M., KONDO, T., KOMODA, M., IKEDA, S., SHINOHARA, K., TANAKA, A., KONDO, J.N. and DOMEN, K., 1998. Cu2O as a photocatalyst for overall water splitting under visible light irradiation. *Chemistry Communications*, , pp. 357-358.

HAU NG, Y., IWASE, A., KUDO, A. and AMAL, R., 2010. Reducing Graphene Oxide on a Visible-Light BiVO4 Photocatalyst for an Enhanced Photoelectrochemical Water Splitting. *Journal of Physical Chemistry Letters*, 1, pp. 2607-2612.

HE, Y., YAN, F., YU, H., YUAN, S., TONG, Z. and SHENG, G., 2014. Hydrogen production in a light-driven photoelectrochemical cell. *Applied Energy*, 113, pp. 164-168.

HE, X. and BOEHM, R.F., 2009. Direct solar water splitting cell using water, WO3, Pt, and polymer electrolyte membrane. *Energy*, 34(10), pp. 1454-1457.

HIGASHI, M., ABE, R., TERAMURA, K., TAKATA, T., OHTANI, B. and DOMEN, K., 2008. Two Step Water Splitting into H2 and O2 under Visible Light by ATaO2N (A=Ca, Sr, Ba) andWO3 with IO3-/I-Shuttle Redox Mediator. *Chemical Physics Letters*, 452, pp. 120-123.

HITOKI, G., ISHIKAWA, A., TAKATA, T., KONDO, J.N., HARA, M. and DOMEN, K., 2002. Ta_3N_5 as a Novel Visible Light-Driven Photocatalyst (λ<600 nm). *Chemistry Letters*, 31(7), pp. 736-737.

HSU, C. and CHEN, D., 2011. Photoresponse and stability improvement of ZnO nanorod array thin film as a single layer of photoelectrode for photoelectrochemical water splitting. *International Journal of Hydrogen Energy*, 36(24), pp. 15538-15547.

HU, C. and TENG, H., 2010. Structural features of p-type semiconducting NiO as a co-catalyst for photocatalytic water splitting. *Journal of Catalysis*, 272(1), pp. 1-8.

HUANG, C., LIAO, C., WU, C. and WU, J.C.S., 2012. Photocatalytic water splitting to produce hydrogen using multi-junction solar cell with different deposited thin films. *Solar Energy Materials and Solar Cells*, 107, pp. 322-328.

HUANG, L., ZHOU, J., HSU, A. and CHEN, R., 2013. Catalytic partial oxidation of *n*-butanol for hydrogen production over LDH-derived Ni-based catalysts. *International Journal of Hydrogen Energy*, 38(34), pp. 14550-14558.

HUANG, Y., WU, J., WEI, Y., LIN, J. and HUANG, M., 2008. Hydrothermal synthesis of K2La2Ti3O10 and photocatalytic splitting of water. *Journal of Alloys and Compounds*, 456(1–2), pp. 364-367.

IKEDA, S., FUBUKI, M., TAKAHARA, Y.K. and MATSUMURA, M., 2006. Photocatalytic activity of hydrothermally synthesized tantalate pyrochlores for overall water splitting. *Applied Catalysis A: General*, 300(2), pp. 186-190.

IKEDA, S., HIRAO, K., ISHINO, S., MATSUMURA, M. and OHTANI, B., 2006. Preparation of platinized strontium titanate covered with hollow silica and its activity for overall water splitting in a novel phase-boundary photocatalytic system. *Catalysis Today*, 117(1–3), pp. 343-349.

IKUMA, Y. and BESSHO, H., 2007. Effect of Pt concentration on the production of hydrogen by a photocatalyst. *International Journal of Hydrogen Energy*, 32(14), pp. 2689-2692.

INOUE, Y., 2009. Photocatalytic water splitting by RuO2-loaded metal oxides and nitrides with d0- and d10 -related electronic configurations. *Energy and Environmental Science*, 2, pp. 364-386.

INOUE, Y., ASAI, Y. and SAYAMA, K., 1994. Photocatalysts with Tunnel Structures for Decomposition of Water Part 1 .-BaTi,O, , a Pentagonal Prism Tunnel Structure, and its Combination with various Promoters. *Journal of chemistry society faraday transcriptions,* 90(5), pp. 797-802.

INOUE, Y., NIIYAMA, T., ASAI, Y. and SATO, K., 1992. Stable Photocatalytic Activity of BaTi409 Combined with Ruthenium Oxide for Decomposition of Water. *Journal of chemsitry society chemistry communications, ,* pp. 579-580.

ISHII, T., KATO, H. and KUDO, A., 2004. H_2 Evolution from an Aqueous Methanol Solution on $SrTiO_3$ Photocatalysts Codoped with Chromium and Tantalum Ions under Visible Light Irradiation. *Journal of Photochemistry and Photobiology A: Chemistry,* 163(1-2), pp. 181-186.

IWASE, A., KATO, H. and KUDO, A., 2013. The effect of Au cocatalyst loaded on La-doped NaTaO3 on photocatalytic water splitting and O2 photoreduction. *Applied Catalysis B: Environmental,* 136–137(0), pp. 89-93.

JANG, J.S., KIM, H.G. and LEE, J.S., 2012. Heterojunction semiconductors: A strategy to develop efficient photocatalytic materials for visible light water splitting. *Catalysis Today,* 185(1), pp. 270-277.

JEONG, H., KIM, T., KIM, D. and KIM, K., 2006. Hydrogen production by the photocatalytic overall water splitting on : Effect of preparation method. *International Journal of Hydrogen Energy,* 31(9), pp. 1142-1146.

JIANG, W., JIAO, X. and CHEN, D., 2013. Photocatalytic water splitting of surfactant-free fabricated high surface area NaTaO3 nanocrystals. *International Journal of Hydrogen Energy,* 38(29), pp. 12739-12746.

JIN, Z., ZHANG, X., LI, S. and LU, G., 2007. 5.1% Apparent quantum efficiency for stable hydrogen generation over eosin-sensitized CuO/TiO2 photocatalyst under visible light irradiation. *Catalysis Communications,* 8(8), pp. 1267-1273.

JING, D., GUO, L., ZHAO, L., ZHANG, X., LIU, H., LI, M., SHEN, S., LIU, G., HU, X., ZHANG, X., ZHANG, K., MA, L. and GUO, P., 2010. Efficient solar hydrogen production by photocatalytic water splitting: From fundamental study to pilot demonstration. *International Journal of Hydrogen Energy,* 35(13), pp. 7087-7097.

KADOWAKI, H., SAITO, N., NISHIYAMA, H. and INOUE, Y., 2007. RuO_2-loaded Sr^{2+}-doped CeO_2 with d^0 Electronic Configuration as a New Photocatalyst for Overall Water Splitting. *Chemistry Letters,* 36(3), pp. 440-441.

KADOWAKI, H., SAITO, N., NISHIYAMA, H., KOBAYASHI, H., SHIMODAIRA, Y. and INOUE, Y., 2007. Overall Splitting of Water by RuO2-Loaded PbWO4 Photocatalyst with d10s2-d0 Configuration. *Journal of Physical Chemistry,* 111, pp. 439-444.

KASAHARA, A., NUKUMIZU, K., HITOKI, G., TAKATA, T., KONDO, J.N., HARA, M., KOBAYASHI, H. and DOMEN, K., 2002. Photoreactions on LaTiO2N under Visible Light Irradiation. *Journal of Physical Chemistry A,* 106, pp. 6750-6753.

KATO, H., ASAKURA, K. and KUDO, A., 2003. Highly Efficient Water Splitting into H2 and O2 over Lanthanum-Doped NaTaO3 Photocatalysts with High Crystallinity and Surface Nanostructure. *Journal of American Chemistry Society,* 125, pp. 3082-3089.

KATO, H., HORI, M., KONTA, H., SHIMODAIRA, Y. and KUDO, A., 2004. Construction of Z-Scheme-Type Heterogeneous Photocatalysis Systems for Water Splitting into H_2 and O_2 under Visible Light Irradiation. *Chemistry Letters,* 33(10), pp. 1348-1349.

KATO, H. and KUDO, A., 2003. Photocatalytic water splitting into H2 and O2 over various tantalate photocatalysts. *Catalysis Today,* 78, pp. 561-569.

KATO, H. and KUDO, A., 2002. Visible-Light-Response and Photocatalytic Activities of TiO_2 and $SrTiO_3$ Photocatalysts Codoped with Antimony and Chromium. *Journal of Physical Chemistry B,* 106(19), pp. 5029-5034.

KATO, H. and KUDO, A., 2001. Energy structure and photocatalytic activity for water splitting of Sr2(Ta1−XNbX)2O7 solid solution. *Journal of Photochemistry and Photobiology A: Chemistry,* 145(1–2), pp. 129-133.

KATO, H., SASAKI, Y., IWASE, A. and KUDO, A., 2007. Role of Iron Ion Electron Mediator on Photocatalytic Overall Water Splitting under Visible Light Irradiation using Z-Scheme Systems. *Chemistry society Japan,* 80(12), pp. 2457-2464.

KHAN, Z. and QURESHI, M., 2012. Tantalum doped BaZrO3 for efficient photocatalytic hydrogen generation by water splitting. *Catalysis Communications,* 28(0), pp. 82-85.

KIM, H.S., KIM, Y.H., AHN, B.T., LEE, J.G., PARK, C.S. and BAE, K.K., 2014. Phase separation characteristics of the Bunsen reaction when using HI_x solution ($HI–I_2–H_2O$) in the sulfur–iodine hydrogen production process. *International Journal of Hydrogen Energy,* 39(2), pp. 692-701.

KIM, H.G., HWANG, W.,DONG, KIM, J., KIM, Y. and LEE, J.S., 1999. Highly donor-doped (110) layered perovskite materials as novel photocatalysts for overall water splitting. *Chemistry Communications,* , pp. 1077-1078.

KIM, S.H., PARK, S., LEE, C.W., HAN, B.S., SEO, S.W., KIM, J.S., CHO, I.S. and HONG, K.S., 2012. Photophysical and photocatalytic water splitting performance of stibiotantalite type-structure compounds, SbMO4 (M = Nb, Ta). *International Journal of Hydrogen Energy,* 37(22), pp. 16895-16902.

KITANO, M., TAKEUCHI, M., MATSUOKA, M., THOMAS, J.M. and ANPO, M., 2007. Photocatalytic water splitting using Pt-loaded visible light-responsive TiO2 thin film photocatalysts. *Catalysis Today,* 120(2), pp. 133-138.

KONTA, R., ISHII, T., KATO, H. and KUDO, A., 2004. Photocatalytic Activities of Noble Metal Ion-doped $SrTiO_3$ Under Visible Light Irradiation. *Journal of Physical Chemistry B,* 108, pp. 8992-8995.

KUDO, A. and KATO, H., 2000. E€ect of lanthanide-doping into NaTaO3 photocatalysts for efficient water splitting. *Chemical Physics Letters,* pp. 373-377.

KUDO, A. and MISEKI, Y., 2009. Heterogeneous photocatalyst materials for water splitting. *The Royal Society of Chemistry,* 38, pp. 253-278.

KUDO, A., TANAKA, A., DOMEN, K. and ONISHI, T., 1988. The effects of the calcination temperature of SrTiO3 powder on photocatalytic activities. *Journal of Catalysis,* 111(2), pp. 296-301.

KUMAR, K., ROY, S. and DAS, D., 2013. Continuous mode of carbon dioxide sequestration by *C. sorokiniana* and subsequent use of its biomass for hydrogen production by *E. cloacae* IIT-BT 08. *Bioresource Technology,* 145, pp. 116-122.

LAI, C.W. and SREEKANTAN, S., 2013. Fabrication of WO3 nanostructures by anodization method for visible-light driven water splitting and photodegradation of methyl orange. *Materials Science in Semiconductor Processing,* 16(2), pp. 303-310.

LAI, K., ZHU, Y., LU, J., DAI, Y. and HUANG, B., 2013. N- and Mo-doping Bi2WO6 in photocatalytic water splitting. *Computational Materials Science,* 67(0), pp. 88-92.

LEE, K., TIENES, B., WILKER, M., SCHNITZEBAUMER, K. and DUKOVIC, G., 2012. (Ga1-xZnx)(N1-xOx) Nanocrystals: Visible Absorbers with Tunable Composition and Absorption Spectra. *Amercian Chemical Society Nano Letters,* 12, pp. 3268-3272.

LEE, Y., TERASHIMA, H., SHIMODAIRA, Y., TERAMURA, K., HARA, M., KOBAYASHI, H., DOMEN, K. and YASHIMA, M., 2007. Zinc Germanium Oxynitride as a Photocatalyst for Overall Water Splitting under Visible Light. *Journal of Physical Chemistry C,* 111, pp. 1042-1048.

LI, Y., YU, H., SONG, W., LI, G., YI, B. and SHAO, Z., 2011. A novel photoelectrochemical cell with self-organized TiO_2 nanotubes as photoanodes for hydrogen generation. *International Journal of Hydrogen Energy,* 36(22), pp. 14374-14380.

LI, Y., YU, H., ZHANG, C., SONG, W., LI, G., SHAO, Z. and YI, B., 2013. Effect of water and annealing temperature of anodized TiO_2 nanotubes on hydrogen production in photoelectrochemical cell. *Electrachimica Acta,* 107, pp. 313-319.

LI, W., LI, J., WANG, X. and CHEN, Q., 2012. Preparation and water-splitting photocatalytic behavior of S-doped WO3. *Applied Surface Science,* 263(0), pp. 157-162.

LI, Y., WU, J., HUANG, Y., HUANG, M. and LIN, J., 2009. Photocatalytic water splitting on new layered perovskite A2.33Sr0.67Nb5O14.335 (A = K, H). *International Journal of Hydrogen Energy,* 34(19), pp. 7927-7933.

LI, Y., CHEN, G., ZHANG, H. and LI, Z., 2009. Electronic structure and photocatalytic water splitting of lanthanum-doped Bi2AlNbO7. *Materials Research Bulletin,* 44(4), pp. 741-746.

LI, Y., CHEN, G., ZHANG, H. and LI, Z., 2009. Photocatalytic water splitting of La2AlTaO7 and the effect of aluminum on the electronic structure. *Journal of Physics and Chemistry of Solids,* 70(3–4), pp. 536-540.

LIANOS, P., 2011. Production of electricity and hydrogen by photocatalytic degradation of organic wastes in a photoelectrochemical cell: The concept of the Photofuelcell: A review of a re-emerging research field. *Journal of Hazardous Materials,* 185(2-3), pp. 575-590.

LIAO, C., HUANG, C. and WU, J.C.S., 2012. Hydrogen production from semiconductor-based photocatalysis via water splitting. *Catalysts,* 2, pp. 490-516.

LIAO, C., HUANG, C. and WU, J.C.S., 2012. Novel dual-layer photoelectrode prepared by RF magnetron sputtering for photocatalytic water splitting. *International Journal of Hydrogen Energy,* 37(16), pp. 11632-11639.

LIBERATORE, R., LANCHI, M., CAPUTO, G., FELICI, C., GIACONIA, A., SAU, S. and TARQUINI, P., 2012. Hydrogen production by flue gas through sulfur–iodine thermochemical process: Economic and energy evaluatio. *International Journal of Hydrogen Energy,* 37(11), pp. 8939-8953.

LIN, H. and CHANG, Y., 2010. Photocatalytic water splitting for hydrogen production on Au/KTiNbO5. *International Journal of Hydrogen Energy,* 35(16), pp. 8463-8471.

LIN, H., CHEN, Y. and CHEN, Y., 2007. Water splitting reaction on NiO/InVO4 under visible light irradiation. *International Journal of Hydrogen Energy,* 32(1), pp. 86-92.

LIN, H., LEE, T. and SIE, C., 2008. Photocatalytic hydrogen production with nickel oxide intercalated K4Nb6O17 under visible light irradiation. *International Journal of Hydrogen Energy,* 33(15), pp. 4055-4063.

LIU, H., YUAN, J., JIANG, Z., SHANGGUAN, W., EINAGA, H. and TERAOKA, Y., 2012. Roles of Bi, M and VO4 tetrahedron in photocatalytic properties of novel Bi0.5M0.5VO4 (M=La, Eu, Sm and Y) solid solutions for overall water splitting. *Journal of Solid State Chemistry,* 186(0), pp. 70-75.

LIU, J., LIU, J. and LI, Z., 2013. Preparation and photocatalytic activity for water splitting of Pt–Na2Ta2O6 nanotube arrays. *Journal of Solid State Chemistry,* 198(0), pp. 192-196.

LIU, S. and SYU, H., 2012. One-step fabrication of N-doped mesoporous TiO2 nanoparticles by self-assembly for photocatalytic water splitting under visible light. *Applied Energy,* 100(0), pp. 148-154.

LIU, Y., XIE, L., LI, Y., YANG, R., QU, J., LI, Y. and LI, X., 2008. Synthesis and high photocatalytic hydrogen production of SrTiO3 nanoparticles from water splitting under UV irradiation. *Journal of Power Sources,* 183(2), pp. 701-707.

LO, C., HUANG, C., LIAO, C. and WU, J.C.S., 2010. Novel twin reactor for separate evolution of hydrogen and oxygen in photocatalytic water splitting. *International Journal of Hydrogen Energy,* 35(4), pp. 1523-1529.

MAEDA, K., HIGASHI, M., LU, D., ABE, R. and DOMEN, K., 2010. Efficient Nonsacrificial Water Splitting through Two-Step Photoexcitation by Visible Light using a Modified Oxynitride as a Hydrogen Evolution Photocatalyst. *Journal of American Chemistry Society,* 132, pp. 5858-5868.

MAEDA, K., 2011. Photocatalytic water splitting using semiconductor particles: History and recent developments. *Journal of Photochemistry and Photobiology C: Photochemistry Reviews,* 12(4), pp. 237-268.

MAEDA, K., TAKATA, T., HARA, M., SAITO, N., INOUE, Y., KOBAYASHI, H. and DOMEN, K., 2005. GaN:ZnO Solid Solution as a Photocatalyst for Visible Light Driven Overall Water Splittin. *Journal of American Chemistry Society,* 127, pp. 8286-8287.

MAEDA, K., TERAMURA, K., SAITO, N., INOUE, Y. and DOMEN, K., 2006. Improvement of photocatalytic activity of (Ga1−xZnx)(N1−xOx) solid solution for overall water splitting by co-loading Cr and another transition metal. *Journal of Catalysis,* 243(2), pp. 303-308.

MAEDA, K., TERAMURA, K., TAKATA, T., HARA, M., SAITO, N., TODA, K., INOUE, Y., KOBAYASHI, H. and DOMEN, K., 2005. Overall Water Splitting on (Ga1-xZnx)(N1-xOx) Solid Solution Photocatalyst: Relationship between Physical Properties and Photocatalytic Activity. *Journal of Physical Chemistry B,* 109(43), pp. 20504-20510.

MATSUMOTO, H., MASHIMO, H. and KURODA, C., 2012. Process Analysis of Rotary-Type Solar Reactor for Hydrogen Production Systems. *Computer Aided Chemical Engineering*, 30, pp. 1103-1107.

MINGGU, L.J., WAN DAUD, W.R. and KASSIM, M., 2010. An overview of photocells and photoreactors for photoelectrochemical water splitting. *International Journal of Hydrogen Energy*, 35(11), pp. 5233-5244.

MISHRA, P.R., SHUKLA, P.K. and SRIVASTAVA, O.N., 2007. Study of modular PEC solar cells for photoelectrochemical splitting of water employing nanostructured TiO_2 photoelectrodes. *International Journal of Hydrogen Energy*, 32(12), pp. 1680-1685.

MIZUKOSHI, Y., MAKISE, Y., SHUTO, T., HU, J., TOMINAGA, A., SHIRONITA, S. and TANABE, S., 2007. Immobilization of noble metal nanoparticles on the surface of TiO2 by the sonochemical method: Photocatalytic production of hydrogen from an aqueous solution of ethanol. *Ultrasonics Sonochemistry*, 14(3), pp. 387-392.

MORADOUR, A., AMOUYAL, E., KELLER, P. and KAGAN, H., 1978. Hydrogen production by visible light irradiation of aqueous solutions of Ru(bipy)32+. *New Journal of Chemistry*, 2(6), pp. 547-549.

MORIYA, Y., TAKATA, T. and DOMEN, K., 2013. Recent progress in the development of (oxy)nitride photocatalysts for water splitting under visible-light irradiation. *Coordination Chemistry Reviews*, 257(13–14), pp. 1957-1969.

MUSA, A., AL-SALEH, M., LOAKEIMIDIS, Z.C., OUZOUNIDOU, M., YENTEKAKIS, I.V., KONSOLAKIS, M. and MARNELLOS, G.E., 2014. Hydrogen production by iso-octane steam reforming over Cu catalysts supported on rare earth oxides (REOs). *International Journal of Hydrogen Energy*, 39(3), pp. 1350-1363.

NAVARRO, R.M., DEL VALLE, F., VILLORIA DE LA MANO, J.A., ÁLVAREZ-GALVÁN, M.C. and FIERRO, J.L.G., Photocatalytic Water Splitting Under Visible Light: Concept and Catalysts Development. *Advances in Chemical Engineering.* Academic Press, pp. 111-143.

OGURA, S., KOHNO, M., SATO, K. and INOUE, Y., 1998. Photocatalytic properties of M2Ti6O13 (M= Na, K, Rb, Cs) with rectangular tunnel and layer structures: Behavior of a surface radical produced by UV irradiation and photocatalytic activity for water decomposition. *Physical chemistry chemical physics*, 1, pp. 179-183.

OHTANI, B., 2008. Preparing Articles on Photocatalysis—Beyond the Illusions, Misconceptions, and Speculation. *Chemistry Letters*, 37(3), pp. 217-229.

PAI, M.R., BANERJEE, A.M., TRIPATHI, A.K. and BHARADWAJ, S.R., 2012. 14 - Fundamentals and Applications of the Photocatalytic Water Splitting Reaction. In: S. BANERJEE and A. TYAGI, eds, *Functional Materials.* London: Elsevier, pp. 579-606.

PUANGPETCH, T., SREETHAWONG, T., YOSHIKAWA, S. and CHAVADEJ, S., 2009. Hydrogen production from photocatalytic water splitting over mesoporous-assembled SrTiO3 nanocrystal-based photocatalysts. *Journal of Molecular Catalysis A: Chemical*, 312(1–2), pp. 97-106.

RAO, P.M., CHO, I.S. and ZHENG, X., 2013. Flame synthesis of WO3 nanotubes and nanowires for efficient photoelectrochemical water-splitting. *Proceedings of the Combustion Institute*, 34(2), pp. 2187-2195.

RAYALU, S.S., DUBEY, N., LABHSETWAR, N.K., KAGNE, S. and DEVOTTA, S., 2007. UV and visibly active photocatalysts for water splitting reaction. *International Journal of Hydrogen Energy*, 32(14), pp. 2776-2783.

REDDY, R.V., HWANG, W.,DONG and LEE, J.S., 2003. Photocatalytic Water Splitting over ZrO2 Prepared by Precipitation Method. *Korean Journal of Chemical Engineering*, 20(6), pp. 1026-1029.

SAKATA, Y., MATSUDA, Y., YANAGIDA, T., HIRATA, K., IMAMURA, H. and TERAMURA, K., 2008. Effect of Metal Ion Addition in a Ni Supported Ga2O3 Photocatalyst on the Photocatalytic Overall Splitting of H2O. *Catalysis Letters*, 125, pp. 22-26.

SASAKI, Y., IWASE, A., KATO, H. and KUDO, A., 2008. The effect of cocatalyst for Z-scheme photocatalysis systems with an Fe^{3+}/Fe^{2+} electron mediator on overall water splitting under visible light irradiation. *Journal of Catalysis*, 259, pp. 133-137.

SASAKI, Y., NEMOTO, H., SAITO, K. and KUDO, A., 2009. Solar Water Splitting Using Powdered Photocatalysts Driven by Z-Schematic Interparticle Electron Transfer without an Electron Mediator. *Journal of Physical Chemistry C*, 113, pp. 17536-17542.

SATO, J., SAITO, N., NISHIYAMA, H. and INOUE, Y., 2002. Photocatalytic water decomposition by RuO2-loaded antimonates, M2Sb2O7 (M=Ca, Sr), CaSb2O6 and NaSbO3, with d10 configuration. *Journal of Photochemistry and Photobiology A: Chemistry*, 148(1–3), pp. 85-89.

SAYAMA, K., ARAKAWA, H. and DOMEN, K., 1996. Photocatalytic water splitting on nickel intercalated A4TaxNb6-xO17 (A = K, Rb). *Catalysis Today*, 28(1–2), pp. 175-182.

SAYAMA, K. and ARAKAWA, H., 1997. Effect of carbonate salt addition on the photocatalytic decomposition of liquid water over Pt–TiO2 catalyst. *Journal of chemistry society faraday transcriptions*, 93(8), pp. 1647-1654.

SAYAMA, K., ARAKAWA, H., ASAKURA, K., TANAKA, A., DOMEN, K. and ONISHI, T., 1998. Photocatalytic activity and reaction mechanism of Pt-interlaced K4Nb6O17 catalyst on the water splitting in carbonate salt aqueous solution. *Journal of Photochemistry and Photobiology A: Chemistry*, 114, pp. 125-135.

SAYAMA, K., MUKASA, K., ABE, R., ABE, Y. and ARAKAWA, H., 2002. A new photocatalytic water splitting system under visible light irradiation mimicking a Z-scheme mechanism in photosynthesis. *Journal of Photochemistry and Photobiology A: Chemistry*, 148(1–3), pp. 71-77.

SAYAMA, K., MUKASA, K., ABE, R., ABE, Y. and ARAKAWA, H., 2001. Stoichiometric water splitting into H2 and O2 using a mixture of two different photocatalysts and an IO3-/I- shuttle redox mediator under visible light irradiation. *Chemical Communications*, 7(23), pp. 2416-2417.

SAYAMA, K., YOSHIDA, M., KUSAMA, H., OKABE, K., ABE, Y. and ARAKAWA, H., 1997. Photocatalytic decomposition of water into H_2 and O_2 by a two-step photoexcitation reaction using a WO_3 suspension catalyst and an $Fe^{3+}Fe^{2+}$ redox system. *Chemical Physics Letters*, 277(4), pp. 387-391.

SHIN, K., YOO, J. and HYEOK, J.P., 2013. Photoelectrochemical cell/dye-sensitized solar cell tandem water splitting systems with transparent and vertically aligned quantum dot sensitized TiO_2 nanorod arrays. *Journal of Power Sources*, 225, pp. 263-268.

SUGAI, Y., PURWASENA, I.A., SASAKI, K., FUJIWARA, K., HATTORI, Y. and OKATSU, K., Journal of Natural Gas Science and Engineering. Experimental studies on indigenous hydrocarbon-degrading and hydrogen-producing bacteria in an oilfield for microbial restoration of natural gas deposits with CO_2 sequestration. *2012,* 5, pp. 31-41.

TABATA, M., MAEDA, K., HIGASHI, M., LU, D., TAKATA, T., ABE, R. and DOMEN, K., 2010. Modified Ta3N5 Powder as a Photocatalyst for O_2 Evolution in a Two-Step Water Splitting System with an Iodate/Iodide Shuttle Redox Mediator under Visible Light. *Langmuir,* 26, pp. 9161-9165.

TAKAHASHI, T., KAKIHANA, M., YAMASHITA, K., YOSHIDA, K., IKEDA, S., HARA, M. and DOMEN, K., 1999. Synthesis of NiO-loaded KTiNbO5 Photocatalysts by a Novel Polymerizable Complex Method. *Journal of Alloys and Compounds,* 285, pp. 77-81.

TAKATA, T., SHINOHARA, K., TANAKA, A., HARA, M., KONDO, J.N. and DOMEN, K., 1997. A highly active photocatalyst for overall water splitting with a hydrated layered perovskite structure. *Journal of Photochemistry and Photobiology A: Chemistry,* 106(1–3), pp. 45-49.

TANG, X., YE, H., LIU, H., MA, C. and ZHAO, Z., 2010. Photocatalytic splitting of water under visible-light irradiation over the NiOx-loaded Sm2InTaO7 with 4f-d10-d0 configuration. *Journal of Solid State Chemistry,* 183(1), pp. 192-197.

TORRES-MARTÍNEZ, L.M., GÓMEZ, R., VÁZQUEZ-CUCHILLO, O., JUÁREZ-RAMÍREZ, I., CRUZ-LÓPEZ, A. and ALEJANDRE-SANDOVAL, F.J., 2010. Enhanced photocatalytic water splitting hydrogen production on RuO2/La:NaTaO3 prepared by sol–gel method. *Catalysis Communications,* 12(4), pp. 268-272.

WANG, G., LING, Y., WANG, H., XIHONG, L. and LI , Y., 2014. Chemically modified nanostructures for photoelectrochemical water splitting. *Journal of Photochemistry and Photobiology C: Photochemistry Reviews,* 19, pp. 35-51.

WANG, B., LI, C., HIRABAYASHI, D. and SUZUKI, K., 2010. Hydrogen evolution by photocatalytic decomposition of water under ultraviolet–visible irradiation over K2La2Ti3−xMxO10+δ perovskite. *International Journal of Hydrogen Energy,* 35(8), pp. 3306-3312.

WANG, Q., AN, N., CHEN, W., WANG, R., WANG, F., LEI, Z. and SHANGGUAN, W., 2012. Photocatalytic water splitting into hydrogen and research on synergistic of Bi/Sm with solid solution of Bi–Sm–V photocatalyst. *International Journal of Hydrogen Energy,* 37(17), pp. 12886-12892.

WANG, Q., AN, N., MU, R., LIU, H., YUAN, J., SHI, J. and SHANGGUAN, W., 2012. Photocatalytic water splitting by band-gap engineering of solid solution Bi1−xDyxVO4 and Bi0.5M0.5VO4 (M = La, Sm, Nd, Gd, Eu, Y). *Journal of Alloys and Compounds,* 522(0), pp. 19-24.

WANG, R., ZHU, Y., QIU, Y., LEUNG, C., HE, J., LIU, G. and LAU, T., 2013. Synthesis of nitrogen-doped KNbO3 nanocubes with high photocatalytic activity for water splitting and degradation of organic pollutants under visible light. *Chemical Engineering Journal,* 226(0), pp. 123-130.

WANG, Y., GUO, X., DONG, L., JIN, G., WANG, Y. and GUO, X., 2013. Enhanced photocatalytic performance of chemically bonded SiC-graphene composites for visible-light-driven overall water splitting. *International Journal of Hydrogen Energy,* 38(29), pp. 12733-12738.

WEAVER, E.R., BERRY, W.M., BOHNSON, V.L. and GORDON, B.D., The ferrosilicon process for the generation of hydrogen, Report No. 40. *Annual Report National Advisory Committee for Aeronautics*.

WEI, Y., LI, J., HUANG, Y., HUANG, M., LIN, J. and WU, J., 2009. Photocatalytic water splitting with In-doped H2LaNb2O7 composite oxide semiconductors. *Solar Energy Materials and Solar Cells,* 93(8), pp. 1176-1181.

XING, Z., ZONG, X., PAN, J. and WANG, L., 2013. On the engineering part of solar hydrogen production from water splitting: photoreactor design. *Chemical Engineering Society,* 104, pp. 125-146.

YAMAGUTI, K. and SATO, S., 1985. Photolysis of Water over Metallized Powdered Titanium Dioxide. *Journal of chemistry society faraday transcriptions,* 81, pp. 1237-1246.

YAMAGUTI, K. and SATO, S., 1984. Photolysis of water over platinum/titanium dioxide catalyst. *Nippon Kagaku Kaishi,* 2, pp. 258-263.

YAMASITA, D., TAKATA, T., HARA, M., KONDO, J.N. and DOMEN, K., 2004. Recent progress of visible-light-driven heterogeneous photocatalysts for overall water splitting. *Solid State Ionics,* 172(1–4), pp. 591-595.

YAN, W., ZHENG, C.L., LIU, Y.L. and GUO, L.J., 2011. A novel dual-bed photocatalytic water splitting system for hydrogen production. *International Journal of Hydrogen Energy,* 36(13), pp. 7405-7409.

YAN, S.C., WANG, Z.Q., LI, Z.S. and ZOU, Z.G., 2009. Photocatalytic activities for water splitting of La-doped-NaTaO3 fabricated by microwave synthesis. *Solid State Ionics,* 180(32–35), pp. 1539-1542.

YANG, H., LIU, X., ZHOU, Z. and GUO, L., 2013. Preparation of a novel Cd2Ta2O7 photocatalyst and its photocatalytic activity in water splitting. *Catalysis Communications,* 31(0), pp. 71-75.

YANG, J., YAN, H., WANG, X., WEN, F., WANG, Z., FAN, D., SHI, J. and LI, C., 2012. Roles of cocatalysts in Pt–PdS/CdS with exceptionally high quantum efficiency for photocatalytic hydrogen production. *Journal of Catalysis,* 290(0), pp. 151-157.

YANG, Y., LEE, K., KADO, Y. and SCHMUKI, P., 2012. Nb-doping of TiO2/SrTiO3 nanotubular heterostructures for enhanced photocatalytic water splitting. *Electrochemistry Communications,* 17(0), pp. 56-59.

YE.J, ZOU, Z., ARAKAWA, H., OSHIKIRI, M., SHIMODA, M., MATSUSHITA, A. and SHISHIDO, T., 2002. Correlation of crystal and electronic structures with photophysical properties of water splitting photocatalysts InMO4 (M = V5+, Nb5+, Ta5+). *Journal of Photochemistry and Photobiology A: Chemistry,* 148, pp. 79-83.

YOSHIDA, M., MAEDA, K., LU, D., KUBOTA, J. and DOMEN, K., 2013. Lanthanoid Oxide Layers on Rhodium-Loaded (Ga1-xZnx)(N1-xOx) Photocatalyst as a Modifier for Overall Water Splitting under Visible- Light Irradiation. *Journal of Physical Chemistry C,* 117, pp. 14000-14006.

YOSHIOKA, K., PETRYKIN, V., KAKIHANA, M., KATO, H. and KUDO, A., 2005. The relationship between photocatalytic activity and crystal structure in strontium tantalates. *Journal of Catalysis,* (232), pp. 102-107.

YU, S., HUANG, C., LIAO, C., WU, J.C.S., CHANG, S. and CHEN, K., 2011. A novel membrane reactor for separating hydrogen and oxygen in photocatalytic water splitting. *Journal of Membrane Science,* 382(1-2), pp. 291-299.

ZHANG, C., ZHU, X., LIAO, Q., WANG, Y., LI, J., DING, Y. and WANG, H., 2010. Performance of a groove-type photobioreactor for hydrogen production by immobilized photosynthetic bacteria. *International Journal of Hydrogen Energy,* 35(11), pp. 5284-5292.

ZHANG, H., HUANG, S. and CONIBEER, G., 2012. Study of Photo-cathode Materials for Tandem Photoelectrochemical Cell for Direct Water Splitting. *Energy Procedia,* 22, pp. 10-14.

ZHANG, W., LI, Y., WANG, C., WANG, P. and WANG, Q., 2013. Energy recovery during advanced wastewater treatment: Simultaneous estrogenic activity removal and hydrogen production through solar photocatalysis. *Water Research,* 47(3), pp. 1480-1490.

ZHANG, Z., HOSSAIN, M.F. and TAKAHASHI, T., 2010. Photoelectrochemical water splitting on highly smooth and ordered TiO_2 nanotube arrays for hydrogen generation. *International Journal of Hydrogen Energy,* 35(16), pp. 8528-8535.

ZHENG, C. and WEST, A., 1991. Compound and Solid-solution Formation, Phase Equilibria and Electrical Properties in the Ceramic System Zr02-La2O3-Ta2O5. *Journal of Material Chemistry,* 1(2), pp. 163-167.

ZHU, L., QIANG, Y.H., ZHAO, Y.L. and GU, X.Q., 2013. Double junction photoelectrochemical solar cells based on $Cu_2ZnSnS_4/Cu_2ZnSnSe_4$ thin film as composite photocathode. *Applied Surface Science*.

ZOU, J., ZHANG, L., LUO, S., LENG, L., LUO, X., ZHANG, M., LUO, Y. and GUO, G., 2012. Preparation and photocatalytic activities of two new Zn-doped SrTiO3 and BaTiO3 photocatalysts for hydrogen production from water without cocatalysts loading. *International Journal of Hydrogen Energy,* 37(22), pp. 17068-17077.

ZOU, Z., YE, J. and ARAKAWA, H., 2003. Photocatalytic water splitting into H2 and/or O2 under UV and visible light irradiation with a semiconductor photocatalyst. *International Journal of Hydrogen Energy,* 28(6), pp. 663-669.